ORNL/TM-10224

ornl

OAK RIDGE
NATIONAL
LABORATORY

MARTIN MARIETTA

Global Ion Cyclotron Waves in a Perpendicularly Stratified, One-Dimensional Warm Plasma

E. F. Jaeger
D. B. Batchelor
H. Weitzner

OPERATED BY
MARTIN MARIETTA ENERGY SYSTEMS, INC.
FOR THE UNITED STATES
DEPARTMENT OF ENERGY

Printed in the United States of America. Available from
National Technical Information Service
U.S. Department of Commerce
5285 Port Royal Road, Springfield, Virginia 22161
NTIS price codes—Printed Copy: A04; Microfiche A01

ORNL/TM-10224
Dist. Category UC-20 g

Fusion Energy Division

GLOBAL ION CYCLOTRON WAVES IN A PERPENDICULARLY STRATIFIED, ONE-DIMENSIONAL WARM PLASMA

E. F. Jaeger
D. B. Batchelor

H. Weitzner
Courant Institute of Mathematical Sciences
New York University
New York, N.Y. 10012

DATE PUBLISHED — April 1987

Prepared by the
OAK RIDGE NATIONAL LABORATORY
Oak Ridge, Tennessee 37831
operated by
MARTIN MARIETTA ENERGY SYSTEMS, INC.
for the
U.S. DEPARTMENT OF ENERGY
under contract DE-AC05-84OR21400

CONTENTS

ACKNOWLEDGMENTS

The authors acknowledge very helpful discussions with our colleagues K. Appert, J. Vaclavik, P. L. Colestock, C. N. Lashmore-Davies, A. Fukuyama, H. Romero, and R. D. Ferraro.

This research was sponsored by the Office of Fusion Energy, U.S. Department of Energy, under contract DE-AC05-84OR21400 with Martin Marietta Energy Systems, Inc.

ABSTRACT

The sixth-order wave equation which results from a finite temperature expansion of the Vlasov equation is solved globally in a perpendicularly stratified, one-dimensional slab plasma. The diamagnetic drift and associated anisotropy are included in the unperturbed distribution function to ensure a self-adjoint system. All x-dependence in the plasma pressure and magnetic field is retained along with the electric field parallel to $\vec{B}$. Thus, Landau damping of the ion Bernstein wave is included as well. Because the wave equation is solved implicitly as a two-point boundary value problem, the evanescent short-wavelength Bernstein waves do not grow exponentially as in shooting methods. Solutions to the complete sixth-order partial differential equation are compared to those from an approximate second-order equation based on local dispersion theory. Strong variations occur in the absorption and in the structure of the wave fields as resonance topology is varied.

1. INTRODUCTION

The recent success of ion cyclotron resonance heating (ICRH) experiments around the world has stimulated interest in reliable theoretical models for calculating global ICRH wave fields and power deposition profiles in tokamak, mirror, and stellarator geometries. There are already a number of full-wave two-dimensional (2-D) calculations in which global solutions for the ICRH wave fields are found in the cold plasma limit [1–5]. In these models, the ion cyclotron resonance is resolved by including an ad hoc collision term in the cold plasma conductivity tensor. While the total power absorbed is relatively independent of collisions in these models, the details of the predicted power deposition profiles are strongly dependent on the particular collision model assumed. To correct this deficiency requires a global solution to the warm plasma wave equation [6]. Unfortunately, this turns out to be a formidable task in two dimensions because of the prohibitively large number of mesh points required to resolve the short wavelengths associated with the ion Bernstein wave [6].

Some insight into finite temperature effects can be obtained from idealized one-dimensional (1-D) slab model calculations [7–11] in which the resolution is sufficient to follow the Bernstein waves accurately. Chiu and Mau [6] directly expand the Vlasov equation to second order in gyroradius. Because they ignore all x-dependence except that in the electric field and in the resonant denominator $\omega - k_z v_z - n\Omega$, where $n = 2$, their analysis applies only near the second harmonic resonance. They also point out that in order to treat the fundamental cyclotron resonance ($n = 1$), the diamagnetic drift terms due to gradients in pressure and magnetic field, which are left out of their work, must be retained in the equilibrium distribution function. The authors in Refs [8–10] likewise leave out these diamagnetic drifts, but they nevertheless apply their calculations to the fundamental ion cyclotron resonance and two ion hybrid resonance cases. In Refs [11, 12] some of the drift terms have been included. However, Martin and Vaclavik [13] are the first authors to include all x-dependence and all of the diamagnetic drift terms and associated anisotropy in the unperturbed distribution function. The resulting wave equation is a sixth-order partial differential equation (PDE) that is rigorously self-adjoint.

It is this sixth-order equation which is solved in this paper for the global ion cyclotron resonant frequency (ICRF) wave field and power absorption. Because the equation is solved implicitly as a two-point boundary value problem, the evanescent

short-wavelength Bernstein waves do not grow exponentially as in shooting methods. Of more current interest than the complete sixth-order solutions are various approximate models which may be extendable to two dimensions. We examine one such approximation [14, 15] in which the detailed structure of the Bernstein wave is neglected while the effect of the mode conversion on the fast wave is retained. The wave equation is thus reduced from sixth order to second order and is easily solvable in two dimensions [16]. We study the regions of validity of this model by comparing it to 1-D solutions of the full sixth-order PDE. An alternative approximation is also studied in which ad hoc damping [10] is used to absorb the Bernstein waves before their wavelength becomes prohibitively small.

2. WAVE EQUATION

We consider a perpendicularly stratified, 1-D slab plasma in which the equilibrium quantities are functions of x only and the applied steady-state magnetic field $\vec{B}_0(x)$ is in the $\hat{z}$-direction. The wave fields $\vec{E}$ and $\vec{B}$ are assumed to be small, with harmonic dependences in y, z, and t of the form $\exp[i(k_y y + k_z z - \omega t)]$. Then from Maxwell's equations,

$$\nabla \times \vec{E} = -\frac{\partial \vec{B}}{\partial t} = i\omega \vec{B} \tag{1}$$

$$\nabla \times \frac{\vec{B}}{\mu_0} = \vec{J} + \frac{\partial(\epsilon_0 \vec{E})}{\partial t} = \vec{J}_{\text{ext}} + \sum_s \vec{J}_s - i\omega\epsilon_0 \vec{E} \tag{2}$$

where $\sum_s$ denotes the sum over electron and ion species. Taking the curl of (1) and using (2) to eliminate $\vec{B}$, we have the vector wave equation

$$-\nabla \times \nabla \times \vec{E} + \frac{\omega^2}{c^2}\vec{E} + i\omega\mu_0 \sum_s \vec{J}_s = -i\omega\mu_0 \vec{J}_{\text{ext}} \tag{3}$$

where $\vec{J}_{\text{ext}}$ is the antenna current and $\sum_s \vec{J}_s$ is the plasma current. Following Ref. [13], $\vec{J}_s$ is found in the Appendix to be

$$\vec{J}_s = \left(\overleftrightarrow{\sigma}_s^{(0)} + \overleftrightarrow{\rho}_s^{(1)} + \overleftrightarrow{\tau}_s^{(2)}\right) \cdot \vec{E} + \left[\overleftrightarrow{\sigma}_s^{(1)} + \overleftrightarrow{\rho}_s^{(2)}\right]_U \cdot \frac{\partial \vec{E}}{\partial x} + \frac{\partial}{\partial x}\left(\left[\overleftrightarrow{\sigma}_s^{(1)} + \overleftrightarrow{\rho}_s^{(2)}\right]_L \cdot \vec{E}\right) + \frac{\partial}{\partial x}\left(\overleftrightarrow{\sigma}_s^{(2)} \cdot \frac{\partial \vec{E}}{\partial x}\right) \tag{4}$$

where (dropping the subscript s)

$$\overleftrightarrow{\sigma}^{(0)} = \begin{pmatrix} \sigma_{xx}^{(0)} & \sigma_{xy}^{(0)} & 0 \\ \sigma_{yx}^{(0)} & \sigma_{yy}^{(0)} & 0 \\ 0 & 0 & \sigma_{zz}^{(0)} \end{pmatrix} \qquad \overleftrightarrow{\rho}^{(1)} = \begin{pmatrix} 0 & 0 & \rho_{xz}^{(1)} \\ 0 & 0 & \rho_{yz}^{(1)} \\ \rho_{zx}^{(1)} & \rho_{zy}^{(1)} & 0 \end{pmatrix}$$

$$\overleftrightarrow{\tau}^{(2)} = \begin{pmatrix} \tau_{xx}^{(2)} & \tau_{xy}^{(2)} & 0 \\ \tau_{yx}^{(2)} & \tau_{yy}^{(2)} & 0 \\ 0 & 0 & \tau_{zz}^{(2)} \end{pmatrix} \qquad \left[\overleftrightarrow{\sigma}^{(1)} + \overleftrightarrow{\rho}^{(2)}\right]_U = \begin{pmatrix} 0 & \rho_{xy}^{(2)} & \sigma_{xz}^{(1)} \\ 0 & 0 & \sigma_{yz}^{(1)} \\ 0 & 0 & 0 \end{pmatrix}$$

$$\overleftrightarrow{\sigma}^{(2)} = \begin{pmatrix} \sigma_{xx}^{(2)} & \sigma_{xy}^{(2)} & 0 \\ \sigma_{yx}^{(2)} & \sigma_{yy}^{(2)} & 0 \\ 0 & 0 & \sigma_{zz}^{(2)} \end{pmatrix} \qquad \left[\overleftrightarrow{\sigma}^{(1)} + \overleftrightarrow{\rho}^{(2)}\right]_L = \begin{pmatrix} 0 & 0 & 0 \\ \rho_{yx}^{(2)} & 0 & 0 \\ \sigma_{zx}^{(1)} & \sigma_{zy}^{(1)} & 0 \end{pmatrix}$$

and

$$\sigma_{xx}^{(0)} = \frac{-i\epsilon_0}{2}\left(\widetilde{P}_1 + \widetilde{P}_{-1}\right) \quad ; \quad \sigma_{yy}^{(0)} = \sigma_{xx}^{(0)}$$

$$\sigma_{xy}^{(0)} = \frac{\epsilon_0}{2}\left(\widetilde{P}_1 - \widetilde{P}_{-1}\right) \quad ; \quad \sigma_{yx}^{(0)} = -\sigma_{xy}^{(0)}$$

$$\sigma_{zz}^{(0)} = -i\epsilon_0 \frac{2\omega}{(\alpha k_z)^2}\left(\omega_p^2 + \omega\widetilde{P}_0\right)$$

$$\sigma_{xz}^{(1)} = \frac{-\epsilon_0}{2k_z\Omega}\left[(\omega-\Omega)\,\widetilde{P}_1 - (\omega+\Omega)\,\widetilde{P}_{-1}\right] \quad ; \quad \sigma_{zx}^{(1)} = \sigma_{xz}^{(1)}$$

$$\sigma_{yz}^{(1)} = \frac{-i\epsilon_0}{2k_z\Omega}\left[2\omega\widetilde{P}_0 - (\omega-\Omega)\,\widetilde{P}_1 - (\omega+\Omega)\,\widetilde{P}_{-1}\right] \quad ; \quad \sigma_{zy}^{(1)} = -\sigma_{yz}^{(1)}$$

$$\sigma_{xx}^{(2)} = \frac{i\epsilon_0}{2\Omega^2}\left(P_2 + P_{-2} - P_1 - P_{-1}\right)$$

$$\sigma_{xy}^{(2)} = \frac{-\epsilon_0}{2\Omega^2}\left(P_2 - P_{-2} - 2P_1 + 2P_{-1}\right) \quad ; \quad \sigma_{yx}^{(2)} = -\sigma_{xy}^{(2)}$$

$$\sigma_{yy}^{(2)} = \frac{i\epsilon_0}{2\Omega^2}\left(P_2 + P_{-2} - 3P_1 - 3P_{-1} + 4P_0\right)$$

$$\sigma_{zz}^{(2)} = \frac{i\epsilon_0}{2\Omega^2 k_z^2}\left[(\omega-\Omega)^2\,\widetilde{P}_1 + (\omega+\Omega)^2\,\widetilde{P}_{-1} - 2\omega^2\widetilde{P}_0\right]$$

$$\rho_{xz}^{(1)} = -ik_y\sigma_{yz}^{(1)} \quad ; \quad \rho_{zx}^{(1)} = -\rho_{xz}^{(1)}$$

$$\rho_{yz}^{(1)} = ik_y\sigma_{xz}^{(1)} - \frac{i\epsilon_0}{k_z\Omega}\frac{\partial}{\partial x}\left(\omega_p^2 + \omega\widetilde{P}_0\right) \quad ; \quad \rho_{zy}^{(1)} = \rho_{yz}^{(1)}$$

$$\rho_{xy}^{(2)} = \frac{-\epsilon_0}{2\Omega^2}\Bigg[2k_y\left(P_1 + P_{-1} - 2P_0\right) + \frac{\partial}{\partial x}\left(P_1 - P_{-1}\right) + \frac{\Omega'}{\Omega}\left(P_{-1} - P_1\right)\Bigg] \quad ; \quad \rho_{xy}^{(2)} = \rho_{xy}^{(2)}$$

$$\tau_{xx}^{(2)} = \frac{i\epsilon_0}{2\Omega^2}\left\{-\frac{1}{2}\frac{\partial^2}{\partial x^2}(P_1+P_{-1})\right.$$
$$+\Omega''\left[\frac{1}{\Omega}(P_2+P_{-2}-P_1-P_{-1})+\frac{\partial}{\partial\omega}(P_1-P_{-1})\right]$$
$$+(\Omega')^2\left[\frac{4}{\Omega^2}(P_1+P_{-1}-P_2-P_{-2})+\frac{3}{\Omega}\frac{\partial}{\partial\omega}(P_{-1}-P_1)\right]$$
$$+\frac{\Omega'}{\Omega}\frac{\partial}{\partial x}\left(P_2+P_{-2}-\frac{1}{2}P_1-\frac{1}{2}P_{-1}\right)$$
$$+k_y\frac{\Omega}{\omega}\left[\frac{\partial}{\partial x}(P_1+P_{-1})+\Omega'\frac{\partial}{\partial\omega}(P_1-P_{-1})\right]$$
$$+k_y\frac{\partial}{\partial x}(P_1-P_{-1}-P_2+P_{-2})$$
$$\left.+k_y\Omega'\left[\frac{1}{\Omega}(4P_2-4P_{-2}+5P_{-1}-5P_1)+2\frac{\partial}{\partial\omega}(P_1+P_{-1})\right]\right\}-k_y^2\sigma_{yy}^{(2)}$$

$$\tau_{xy}^{(2)} = \frac{-\epsilon_0}{2\Omega^2}\left\{\frac{1}{2}\frac{\partial^2}{\partial x^2}(P_{-1}-P_1)+\frac{\Omega'}{\Omega}\frac{\partial}{\partial x}\left(P_2-P_{-2}+\frac{1}{2}P_{-1}-\frac{1}{2}P_1\right)\right.$$
$$+\Omega''\left[\frac{1}{\Omega}\left(P_2-P_{-2}+\frac{1}{2}P_{-1}-\frac{1}{2}P_1\right)+\frac{\partial}{\partial\omega}(P_1+P_{-1})\right]$$
$$+(\Omega')^2\left[\frac{1}{\Omega^2}\left(4P_{-2}-4P_2+\frac{7}{2}P_1-\frac{7}{2}P_{-1}\right)-\frac{3}{\Omega}\frac{\partial}{\partial\omega}(P_1+P_{-1})\right]$$
$$+k_y\frac{\partial}{\partial x}(P_1+P_{-1}-P_2-P_{-2})+k_y2\Omega'\left[\frac{\partial}{\partial\omega}(P_1-P_{-1})\right.$$
$$\left.+\frac{1}{\Omega}(2P_0-3P_1-3P_{-1}+2P_2+2P_{-2})\right]$$
$$\left.+k_y\frac{\Omega}{\omega}\left[\frac{\partial}{\partial x}(P_1-P_{-1})+\Omega'\frac{\partial}{\partial\omega}(P_1+P_{-1})\right]\right\}-k_y^2\sigma_{xy}^{(2)}$$

$$\tau_{yx}^{(2)} = -\tau_{xy}^{(2)}$$

$$\tau_{yy}^{(2)} = \frac{i\epsilon_0}{2\Omega^2}\left\{-\frac{3}{2}\frac{\partial^2}{\partial x^2}(P_1+P_{-1}) - 2\frac{\Omega}{\omega}\frac{\partial}{\partial x}\left[\frac{1}{\Omega}\frac{\partial}{\partial x}\left(\frac{\omega_p^2\alpha^2}{2}\right)\right]\right.$$
$$+\Omega''\left[\frac{1}{\Omega}(P_2+P_{-2}+P_1+P_{-1}-4P_0)+\frac{\partial}{\partial\omega}(P_1-P_{-1})\right]$$
$$+(\Omega')^2\left[\frac{3}{\Omega}\frac{\partial}{\partial\omega}(P_{-1}-P_1)+\frac{4}{\Omega^2}(2P_0-P_2-P_{-2})\right]$$
$$+\frac{\Omega'}{\Omega}\frac{\partial}{\partial x}\left(P_2+P_{-2}+\frac{5}{2}P_1+\frac{5}{2}P_{-1}-4P_0\right)$$
$$+k_y\frac{\partial}{\partial x}(P_{-1}-P_1+P_{-2}-P_2)$$
$$+k_y\Omega'\left[2\frac{\partial}{\partial\omega}(P_1+P_{-1})+\frac{1}{\Omega}(4P_2-4P_{-2}-3P_1+3P_{-1})\right]$$
$$\left.+k_y\frac{\Omega}{\omega}\left[\frac{\partial}{\partial x}(P_1+P_{-1})+\Omega'\frac{\partial}{\partial\omega}(P_1-P_{-1})\right]\right\} - k_y^2\sigma_{xx}^{(2)}$$

$$\tau_{zz}^{(2)} = \frac{i\epsilon_0}{2k_z^2}\left\{-\frac{\omega}{\Omega^2}\left[\frac{\partial^2}{\partial x^2}\left(\omega_p^2+\omega\tilde{P}_0\right)+\frac{\Omega'}{\Omega}\frac{\partial}{\partial x}\left(-\omega_p^2-\omega\tilde{P}_0\right)\right]\right.$$
$$-k_y\frac{\partial}{\partial x}\left[\left(\frac{\omega-\Omega}{\Omega}\right)^2\tilde{P}_1-\left(\frac{\omega+\Omega}{\Omega}\right)^2\tilde{P}_{-1}\right]+2k_y\frac{\partial}{\partial x}\left(\frac{1}{\Omega}\right)\frac{\partial}{\partial\omega}\left(\omega^2\tilde{P}_0\right)$$
$$\left.-\frac{2k_y}{\Omega}\frac{\partial}{\partial x}\left(2\omega_p^2+\omega\tilde{P}_0\right)\right\} - k_y^2\sigma_{zz}^{(2)}$$

The superscripts denote order with respect to the ion Larmor radius expansion. The functions $\tilde{P}_n$ and P_n are

$$\tilde{P}_n = \frac{\omega_p^2}{|k_z|\alpha}Z\left(\frac{\omega-n\Omega}{|k_z|\alpha}\right)$$
$$P_n = \frac{\alpha^2}{2}\tilde{P}_n \qquad (5)$$

where α is the thermal speed $\sqrt{2kT/m}$, $\Omega = eB/m$, $\omega_p^2 = ne^2/\epsilon_0 m$, and Z is the plasma dispersion function as defined by Fried and Conte [17],

$$Z(\xi) = \frac{1}{\sqrt{\pi}}\int_{-\infty}^{\infty}dx\frac{e^{-x^2}}{x-\xi} \quad , \quad \mathrm{Im}\ \xi > 0$$
$$= i\sqrt{\pi}e^{-\xi^2} - 2e^{-\xi^2}\int_0^{\xi}dx\ e^{-x^2} \qquad (6)$$

with

$$Z'(\xi) = -2\left[1 + \xi Z(\xi)\right]$$

$$Z''(\xi) = -2\left[Z(\xi) + \xi Z'(\xi)\right]$$

In the limit of large argument, Eq. (6) becomes real, with

$$Z(\xi) \to -\frac{1}{\xi} - \frac{1}{2\xi^3} - \frac{3}{4\xi^5} - \cdots \quad (|\xi| \gg 1)$$

If we now define the dielectric tensors

$$\begin{aligned}
\overleftrightarrow{\epsilon}^{(0)} &= \overleftrightarrow{I} + \frac{i}{\epsilon_0 \omega} \sum_s \overleftrightarrow{\sigma}_s^{(0)} \\
\overleftrightarrow{\epsilon}^{(1,2)} &= \frac{i}{\epsilon_0 \omega} \sum_s \overleftrightarrow{\sigma}_s^{(1,2)} \\
\overleftrightarrow{\delta}^{(n)} &= \frac{i}{\epsilon_0 \omega} \sum_s \overleftrightarrow{\rho}_s^{(n)} \\
\overleftrightarrow{\zeta}^{(n)} &= \frac{i}{\epsilon_0 \omega} \sum_s \overleftrightarrow{\tau}_s^{(n)}
\end{aligned} \tag{7}$$

then Eq. (3) can be written as

$$\begin{aligned}
-\frac{1}{k_0^2}\left(\nabla \times \nabla \times \vec{E}\right) + \left(\overleftrightarrow{\epsilon}^{(0)} + \overleftrightarrow{\delta}^{(1)} + \overleftrightarrow{\zeta}^{(2)}\right) \cdot \vec{E} + \left[\overleftrightarrow{\epsilon}^{(1)} + \overleftrightarrow{\delta}^{(2)}\right]_U \cdot \frac{\partial \vec{E}}{\partial x} \\
+ \frac{\partial}{\partial x}\left(\left[\overleftrightarrow{\epsilon}^{(1)} + \overleftrightarrow{\delta}^{(2)}\right]_L \cdot \vec{E}\right) + \frac{\partial}{\partial x}\left(\overleftrightarrow{\epsilon}^{(2)} \cdot \frac{\partial \vec{E}}{\partial x}\right) = \frac{-i}{\omega \epsilon_0} \vec{J}_{\text{ext}}
\end{aligned} \tag{8}$$

where $k_0 = \omega/c$. The $\hat{x}$, $\hat{y}$, and $\hat{z}$ components of Eq. (8) are:

$$
\begin{aligned}
&\frac{\partial}{\partial x}\left(\epsilon_{xx}^{(2)}\frac{\partial E_x}{\partial x}\right) + \left(-n_y^2 - n_z^2 + \epsilon_{xx}^{(2)} + \varsigma_{xx}^{(2)}\right) E_x + \frac{\partial}{\partial x}\left(\epsilon_{xy}^{(2)}\frac{\partial E_y}{\partial x}\right) \\
&\qquad + \left(\delta_{xy}^{(2)} - \frac{in_y}{k_0}\right)\frac{\partial E_y}{\partial x} + \left(\epsilon_{xy}^{(0)} + \varsigma_{xy}^{(2)}\right) E_y \\
&\qquad + \left(\epsilon_{xz}^{(1)} - \frac{in_z}{k_0}\right)\frac{\partial E_z}{\partial x} + \delta_{xz}^{(1)} E_z = \frac{-i}{\epsilon_0\omega} J_{\text{ext},x} \\
&\frac{\partial}{\partial x}\left(\epsilon_{yx}^{(2)}\frac{\partial E_x}{\partial x}\right) + \frac{\partial}{\partial x}\left[\left(\delta_{yx}^{(2)} - \frac{in_y}{k_0}\right) E_x\right] \\
&\qquad + \left(\epsilon_{yx}^{(0)} + \varsigma_{yx}^{(2)}\right) E_x + \frac{\partial}{\partial x}\left[\left(\epsilon_{yy}^{(2)} + \frac{1}{k_0^2}\right)\frac{\partial E_y}{\partial x}\right] \\
&\qquad + \left(\epsilon_{yy}^{(0)} + \varsigma_{yy}^{(2)} - n_z^2\right) E_y + \epsilon_{yz}^{(1)}\frac{\partial E_z}{\partial x} \\
&\qquad + \left(\delta_{yz}^{(1)} + n_y n_z\right) E_z = -\frac{i}{\epsilon_0\omega} J_{\text{ext},y} \\
&\frac{\partial}{\partial x}\left[\left(\epsilon_{zx}^{(1)} - \frac{in_z}{k_0}\right) E_x\right] + \delta_{zx}^{(1)} E_x + \frac{\partial}{\partial x}\left(\epsilon_{zy}^{(1)} E_y\right) + \left(\delta_{zy}^{(1)} + n_y n_z\right) E_y \\
&\qquad + \frac{\partial}{\partial x}\left[\left(\epsilon_{zz}^{(2)} + \frac{1}{k_0^2}\right)\frac{\partial E_z}{\partial x}\right] + \left(\epsilon_{zz}^{(0)} + \varsigma_{zz}^{(2)} - n_y^2\right) E_z \\
&\qquad = -\frac{i}{\epsilon_0\omega} J_{\text{ext},z}
\end{aligned}
\tag{9}
$$

where $\vec{n} = \vec{k}/k_0$.

3. ENERGY CONSERVATION AND ABSORBED POWER

The equation for energy conservation (Poynting's theorem) is found by dotting $\vec{E}^*$ into the $\nabla \times \vec{B}$ equation in (2),

$$\vec{E}^* \cdot \nabla \times \frac{\vec{B}}{\mu_0} + i\omega\epsilon_0 |E|^2 - \vec{E}^* \cdot \sum_s \vec{J}_s = \vec{E}^* \cdot \vec{J}_{\text{ext}} \tag{10}$$

Now we apply the vector identity

$$\nabla \cdot \vec{B} \times \vec{E}^* = \vec{E}^* \cdot \nabla \times \vec{B} - \vec{B} \cdot \nabla \times \vec{E}^*$$

to the left-hand side of (10) and use (1) to eliminate $\nabla \times \vec{E}^*$. This gives

$$-\frac{1}{\mu_0} \nabla \cdot \left(\vec{E}^* \times \vec{B} \right) + i\omega \left(\epsilon_0 |E|^2 - \frac{|B|^2}{\mu_0} \right) - \vec{E}^* \cdot \sum_s \vec{J}_s = \vec{E}^* \cdot \vec{J}_{\text{ext}}$$

or taking the real part and dividing by (-2.0), we have Poynting's theorem:

$$\boxed{\nabla \cdot \left\{ \frac{1}{2\mu_0} \text{Re} \left(\vec{E}^* \times \vec{B} \right) \right\} + \frac{1}{2} \text{Re} \left\{ \vec{E}^* \cdot \sum_s \vec{J}_s \right\} = -\frac{1}{2} \text{Re} \left\{ \vec{E}^* \cdot \vec{J}_{\text{ext}} \right\}} \tag{11}$$

The first term in (11) is the divergence of Poynting's vector $\vec{S}_p$, where

$$\vec{S}_p = \frac{1}{2\mu_0} \text{Re} \left(\vec{E}^* \times \vec{B} \right)$$

$$S_{p,x} = \frac{1}{2\mu_0 \omega} \text{Im} \left\{ E_y^* \left(\frac{\partial E_y}{\partial x} - ik_y E_x \right) + E_z^* \left(\frac{\partial E_z}{\partial x} - ik_z E_x \right) \right\}$$

The second term in (11) is $1/2$ $\text{Re}\left(\vec{E}^* \cdot \sum_s \vec{J}_s \right)$ and can be written as the sum of the power dissipated $\sum_s P_s$ and the divergence of a kinetic energy flux $\vec{Q}$, which is the energy flux of the wave carried by particle's thermal motion,

$$\frac{1}{2} \text{Re} \left(\vec{E}^* \cdot \sum_s \vec{J}_s \right) = \sum_s P_s + \nabla \cdot \vec{Q} \tag{12}$$

The total energy flux $\vec{S}$ is the sum of the Poynting flux $\vec{S}_p$ and $\vec{Q}$,

$$\vec{S} = \vec{S}_p + \vec{Q}$$

and conservation of energy in (11) takes the form

$$\nabla \cdot \vec{S} + \sum_s P_s = -\frac{1}{2}\mathrm{Re}\left\{E^* \cdot \vec{J}_{\mathrm{ext}}\right\} \tag{13}$$

Now, from (4),

$$\begin{aligned}\frac{1}{2}\mathrm{Re}\left(\vec{E}^\dagger \cdot \sum_s \vec{J}_s\right) = \sum_s \frac{1}{2}\mathrm{Re}\Bigg\{ & \vec{E}^\dagger \cdot \left(\overleftrightarrow{\sigma}_s^{(0)} + \overleftrightarrow{\rho}_s^{(1)} + \overleftrightarrow{\tau}_s^{(2)}\right) \cdot \vec{E} \\ & + E^\dagger \cdot \left[\overleftrightarrow{\sigma}_s^{(1)} + \overleftrightarrow{\rho}_s^{(2)}\right]_U \cdot \frac{\partial \vec{E}}{\partial x} \\ & + E^\dagger \cdot \frac{\partial}{\partial x}\left(\left[\overleftrightarrow{\sigma}_s^{(1)} + \overleftrightarrow{\rho}_s^{(2)}\right]_L \cdot \vec{E}\right) \\ & + E^\dagger \cdot \frac{\partial}{\partial x}\left(\overleftrightarrow{\sigma}_s^{(2)} \frac{\partial \vec{E}}{\partial x}\right)\Bigg\}\end{aligned} \tag{14}$$

where the dagger (†) denotes the transposed complex conjugate or "Hermitian adjoint". If we define

$$\overleftrightarrow{\sigma}_p = \overleftrightarrow{\sigma}_s^{(0)} + \overleftrightarrow{\rho}_s^{(1)} + \overleftrightarrow{\tau}_s^{(2)} + \frac{\partial}{\partial x}\left[\overleftrightarrow{\sigma}_s^{(1)} + \overleftrightarrow{\rho}_s^{(2)}\right]_L$$

$$\overleftrightarrow{\sigma}_Q \equiv \left[\overleftrightarrow{\sigma}_s^{(1)} + \overleftrightarrow{\rho}_s^{(2)}\right]_U + \left[\overleftrightarrow{\sigma}_s^{(1)} + \overleftrightarrow{\rho}_s^{(2)}\right]_L = \begin{pmatrix} 0 & \rho_{xy}^{(2)} & \sigma_{xz}^{(1)} \\ \rho_{xy}^{(2)} & 0 & \sigma_{yz}^{(1)} \\ \sigma_{xz}^{(1)} & -\sigma_{yz}^{(1)} & 0 \end{pmatrix}$$

then Eq. (14) can be written more concisely as

$$\begin{aligned}\frac{1}{2}\mathrm{Re}\left(\vec{E}^\dagger \cdot \sum_s \vec{J}_s\right) = \sum_s \frac{1}{2}\mathrm{Re}\Bigg\{ & \vec{E}^\dagger \cdot \overleftrightarrow{\sigma}_p \cdot \vec{E} \\ & + \vec{E}^\dagger \cdot \overleftrightarrow{\sigma}_Q \cdot \frac{\partial \vec{E}}{\partial x} + \vec{E}^\dagger \cdot \frac{\partial}{\partial x}\left(\overleftrightarrow{\sigma}_s^{(2)} \frac{\partial \vec{E}}{\partial x}\right)\Bigg\} \\ = \sum_s P_s + \frac{\partial Q_x}{\partial x}\end{aligned} \tag{15}$$

Written out explicitly, Eq. (15) gives

$$\begin{aligned}
\frac{1}{2}\mathrm{Re}\left(\vec{E}^{\dagger}\cdot\sum_s \vec{J}_s\right) = \sum_s \frac{1}{2}\mathrm{Re}\Bigg\{ & E_x^*\Bigg[\left(\sigma_{xx}^{(0)}+\tau_{xx}^{(2)}\right)E_x \\
& + \left(\sigma_{xy}^{(0)}+\tau_{xy}^{(2)}\right)E_y + \rho_{xz}^{(1)}E_z + \rho_{xy}^{(2)}\frac{\partial E_y}{\partial x} \\
& + \sigma_{xz}^{(1)}\frac{\partial E_z}{\partial x} + \frac{\partial}{\partial x}\left(\sigma_{xx}^{(2)}\frac{\partial E_x}{\partial x}+\sigma_{xy}^{(2)}\frac{\partial E_y}{\partial x}\right)\Bigg] \\
& + E_y^*\Bigg[\left(-\sigma_{xy}^{(0)}-\tau_{xy}^{(2)}+\frac{\partial \rho_{xy}^{(2)}}{\partial x}\right)E_x \\
& + \left(\sigma_{yy}^{(0)}+\tau_{yy}^{(2)}\right)E_y + \rho_{yz}^{(1)}E_z + \rho_{xy}^{(2)}\frac{\partial E_x}{\partial x} + \sigma_{yz}^{(1)}\frac{\partial E_z}{\partial x} \\
& + \frac{\partial}{\partial x}\left(-\sigma_{xy}^{(2)}\frac{\partial E_x}{\partial x}+\sigma_{yy}^{(2)}\frac{\partial E_y}{\partial x}\right)\Bigg] \\
& + E_z^*\Bigg[\left(-\rho_{xz}^{(1)}+\frac{\partial \sigma_{xz}^{(1)}}{\partial x}\right)E_x + \left(\rho_{yz}^{(1)}-\frac{\partial \sigma_{yz}^{(1)}}{\partial x}\right)E_y \\
& + \left(\sigma_{zz}^{(0)}+\tau_{zz}^{(2)}\right)E_z + \sigma_{xz}^{(1)}\frac{\partial E_x}{\partial x} - \sigma_{yz}^{(1)}\frac{\partial E_y}{\partial x} \\
& + \frac{\partial}{\partial x}\left(\sigma_{zz}^{(2)}\frac{\partial E_z}{\partial x}\right)\Bigg]\Bigg\}
\end{aligned} \tag{16}$$

Using Eq. (16), we have checked the conservation of energy [Eq. (11)] in our numerical calculation. We find that except at the antenna where $\vec{J}_{\mathrm{ext}} \neq 0$, the two terms on the left-hand side of Eq. (11) are to a good approximation equal and opposite in sign. Thus, Poynting's theorem is satisfied locally to a high degree of accuracy in our numerical solutions. Nevertheless, a problem arises in the definition of the kinetic flux $\vec{Q}$. A unique determination of $\vec{Q}$ requires carrying the calculation to second order in the perturbing wave field. For a first-order, linear calculation such as this one, the choice of $\vec{Q}$ is not unique. Thus, there are a number of different definitions for $\vec{Q}$ occurring in the literature [6,11,13]. Here we choose $\vec{Q}$ to ensure consistency with the WKB result in the weak damping limit for a single wave. Thus, we take

$$Q_x = \sum_s \frac{1}{2}\,\mathrm{Re}\left\{\vec{E}^{\dagger}\cdot\frac{\overleftrightarrow{\sigma}_{Q,H}}{2}\cdot\vec{E} + \vec{E}^{\dagger}\cdot\overleftrightarrow{\sigma}^{(2)}\cdot\frac{\partial\vec{E}}{\partial x}\right\} \tag{17}$$

where the subscripts H and A denote the Hermitian and anti-Hermitian parts, respectively:

$$\sigma_{Hij} \equiv \frac{1}{2}\left(\sigma_{ij} + \sigma_{ji}^*\right)$$

$$\sigma_{Aij} \equiv \frac{1}{2}\left(\sigma_{ij} - \sigma_{ji}^*\right)$$

With these definitions, it can be shown that

$$\mathrm{Re}\left(\vec{E}^\dagger \cdot \overleftrightarrow{\sigma}_A \cdot \vec{E}\right) = 0$$

$$\mathrm{Re}\left(\vec{E}^\dagger \cdot \overleftrightarrow{\sigma} \cdot \vec{E}\right) = \mathrm{Re}\left(\vec{E}^\dagger \cdot \overleftrightarrow{\sigma}_H \cdot \vec{E}\right)$$

$$\mathrm{Re}\frac{\partial}{\partial x}\left(\vec{E}^\dagger \cdot \overleftrightarrow{\sigma} \cdot \vec{E}\right) = 2\mathrm{Re}\left(\vec{E}^\dagger \cdot \overleftrightarrow{\sigma}_H \cdot \frac{\partial \vec{E}}{\partial x}\right) + \mathrm{Re}\left(\vec{E}^\dagger \cdot \frac{\partial \overleftrightarrow{\sigma}_H}{\partial x} \cdot \vec{E}\right)$$

$$2\mathrm{Re}\left(\vec{E}^\dagger \cdot \overleftrightarrow{\sigma}_H \cdot \frac{\partial \vec{E}}{\partial x}\right) = \mathrm{Re}\left\{\vec{E}^\dagger \cdot \overleftrightarrow{\sigma} \cdot \frac{\partial \vec{E}}{\partial x} + \frac{\partial \vec{E}^\dagger}{\partial x} \cdot \overleftrightarrow{\sigma} \cdot \vec{E}\right\}$$

$$2\mathrm{Re}\left(\vec{E}^\dagger \cdot \overleftrightarrow{\sigma}_A \cdot \frac{\partial \vec{E}}{\partial x}\right) = \mathrm{Re}\left\{\vec{E}^\dagger \cdot \overleftrightarrow{\sigma} \cdot \frac{\partial \vec{E}}{\partial x} - \frac{\partial \vec{E}^\dagger}{\partial x} \cdot \overleftrightarrow{\sigma} \cdot \vec{E}\right\}$$

Using the identities in (15), the divergence of Q_x is

$$\frac{\partial Q_x}{\partial x} = \sum_s \frac{1}{2}\mathrm{Re}\left\{\vec{E}^\dagger \cdot \overleftrightarrow{\sigma}_{Q,H} \cdot \frac{\partial \vec{E}}{\partial x} + \vec{E}^\dagger \cdot \frac{1}{2}\frac{\partial \overleftrightarrow{\sigma}_{Q,H}}{\partial x} \cdot \vec{E} + \vec{E}^\dagger \cdot \frac{\partial}{\partial x}\left(\overleftrightarrow{\sigma}^{(2)} \cdot \frac{\partial \vec{E}}{\partial x}\right) + \frac{\partial \vec{E}^\dagger}{\partial x} \cdot \overleftrightarrow{\sigma}^{(2)} \cdot \frac{\partial \vec{E}}{\partial x}\right\} \tag{18}$$

Now subtracting (18) from (15) gives for P_s

$$P_s = \frac{1}{2}\mathrm{Re}\left\{\vec{E}^\dagger \cdot \left(\overleftrightarrow{\sigma}_p - \frac{1}{2}\frac{\partial \overleftrightarrow{\sigma}_Q}{\partial x}\right)_H \cdot \vec{E} + \vec{E}^\dagger \cdot \overleftrightarrow{\sigma}_{Q,A} \cdot \frac{\partial \vec{E}}{\partial x} - \frac{\partial \vec{E}^\dagger}{\partial x} \cdot \overleftrightarrow{\sigma}^{(2)} \cdot \frac{\partial \vec{E}}{\partial x}\right\} \tag{19}$$

It is possible to write Q_x and P_s in Eqs (17) and (19) explicitly,

$$\begin{aligned} Q_x = \sum_s \frac{1}{2}\mathrm{Re}\Big\{ & E_x^*\Big(E_y \mathrm{Re}\rho_{xy}^{(2)} + E_z \mathrm{Re}\sigma_{xz}^{(1)}\Big) \\ & + E_x^* \frac{\partial E_x}{\partial x}\sigma_{xx}^{(2)} + E_y^* \frac{\partial E_y}{\partial x}\sigma_{yy}^{(2)} \\ & + E_z^* \frac{\partial E_z}{\partial x}\sigma_{zz}^{(2)} \\ & + \left(E_x^* \frac{\partial E_y}{\partial x} - E_y^* \frac{\partial E_x}{\partial x}\right)\sigma_{xy}^{(2)}\Big\} \\ & - \frac{1}{2}\mathrm{Im}\Big\{ E_y^* E_z \mathrm{Im}\sigma_{yz}^{(1)}\Big\} \end{aligned} \tag{20}$$

$$\begin{aligned} P_s = & \mathrm{Re}\left(\sigma_{xx}^{(0)} + \tau_{xx}^{(2)}\right)\frac{|E_x|^2}{2} + \mathrm{Re}\left(\sigma_{yy}^{(0)} + \tau_{yy}^{(2)}\right)\frac{|E_y|^2}{2} \\ & + \mathrm{Re}\left(\sigma_{zz}^{(0)} + \tau_{zz}^{(2)}\right)\frac{|E_z|^2}{2} \\ & - \frac{1}{2}\,\mathrm{Re}(\sigma_{xx}^{(2)})\left|\frac{\partial E_x}{\partial x}\right|^2 - \frac{1}{2}\,\mathrm{Re}(\sigma_{yy}^{(2)})\left|\frac{\partial E_y}{\partial x}\right|^2 - \frac{1}{2}\,\mathrm{Re}(\sigma_{zz}^{(2)})\left|\frac{\partial E_z}{\partial x}\right|^2 \\ & - \mathrm{Im}\left\{E_x^*\left[E_y \mathrm{Im}\left(\sigma_{xy}^{(0)} + \tau_{xy}^{(2)} - \frac{1}{2}\frac{\partial \rho_{xy}^{(2)}}{\partial x}\right) + E_z \mathrm{Im}\left(\rho_{xz}^{(1)} - \frac{1}{2}\frac{\partial \sigma_{xz}^{(1)}}{\partial x}\right)\right]\right\} \\ & + \mathrm{Re}E_y^* E_z \mathrm{Re}\left(\rho_{yz}^{(1)} - \frac{1}{2}\frac{\partial \sigma_{yz}^{(1)}}{\partial x}\right) \\ & - \frac{1}{2}\mathrm{Im}\left\{\left(E_x^*\frac{\partial E_y}{\partial x} + E_y^*\frac{\partial E_x}{\partial x}\right)\mathrm{Im}\rho_{xy}^{(2)} + \left(E_x^*\frac{\partial E_z}{\partial x} + E_z^*\frac{\partial E_x}{\partial x}\right)\mathrm{Im}\sigma_{xz}^{(1)}\right\} \\ & + \frac{1}{2}\mathrm{Re}\left\{\left(E_y^*\frac{\partial E_z}{\partial x} - E_z^*\frac{\partial E_y}{\partial x}\right)\mathrm{Re}\sigma_{yz}^{(1)}\right\} \\ & + \mathrm{Im}\sigma_{xy}^{(2)}\mathrm{Im}\left(\frac{\partial E_x^*}{\partial x}\frac{\partial E_y}{\partial x}\right) \end{aligned} \tag{21}$$

Note that P_s depends only on the dissipative part of the conductivity. Thus, in the absence of dissipation, the Z functions become real, and the real and imaginary parts of the tensor elements in Eq. (21) are identically zero.

Now consider Eqs (17) and (19) in the WKB limit, that is, in an infinite uniform plasma with B constant and

$$\begin{aligned}\vec{E}(x) &= \varepsilon(\vec{x})e^{ik_x x} \\ \frac{\partial \vec{E}}{\partial x} &= \left(ik_x\vec{\varepsilon} + \frac{\partial \vec{\varepsilon}}{\partial x}\right)e^{ik_x x} \\ \frac{\partial^2 \vec{E}}{\partial x^2} &= \left(-k_x^2\vec{\varepsilon} + 2ik_x\frac{\partial \vec{\varepsilon}}{\partial x} + \frac{\partial^2 \vec{\varepsilon}}{\partial x^2}\right)e^{ik_x x}\end{aligned} \tag{22}$$

Then

$$\begin{aligned}\rho^{(1)} = \quad \rho^{(2)} = \quad \tau^{(2)} &= 0 \\ \frac{\partial \sigma^{(0)}}{\partial x} = \frac{\partial \sigma^{(1)}}{\partial x} = \frac{\partial \sigma^{(2)}}{\partial x} &= 0\end{aligned}$$

and Eqs (4), (17), and (19) give, respectively,

$$\begin{aligned}\vec{J}_s &= \left[\left(\overleftrightarrow{\sigma}^{(0)} + ik_x\overleftrightarrow{\sigma}^{(1)} - k_x^2\overleftrightarrow{\sigma}^{(2)}\right)\cdot\vec{\varepsilon} + \left(\overleftrightarrow{\sigma}^{(1)} + 2ik_x\overleftrightarrow{\sigma}^{(2)}\right)\cdot\frac{\partial \vec{\varepsilon}}{\partial x}\right. \\ &\quad \left. + \overleftrightarrow{\sigma}^{(2)}\cdot\frac{\partial^2 \vec{\varepsilon}}{\partial x^2}\right]e^{ik_x x} \\ Q_x &= \sum_s \frac{1}{2}\mathrm{Re}\left\{\vec{\varepsilon}^{\dagger}\cdot\left(\frac{\overleftrightarrow{\sigma}_H^{(1)}}{2} + ik_x\overleftrightarrow{\sigma}_A^{(2)}\right)\cdot\vec{\varepsilon} + \vec{\varepsilon}^{\dagger}\cdot\overleftrightarrow{\sigma}^{(2)}\cdot\frac{\partial \vec{\varepsilon}}{\partial x}\right\} \\ P_s &= \frac{1}{2}\mathrm{Re}\left\{\varepsilon^{\dagger}\cdot\left(\overleftrightarrow{\sigma}_H^{(0)} + ik_x\overleftrightarrow{\sigma}_A^{(1)} - k_x^2\overleftrightarrow{\sigma}_H^{(2)}\right)\cdot\vec{\varepsilon}\right. \\ &\quad \left. + \vec{\varepsilon}^{\dagger}\cdot\left(\overleftrightarrow{\sigma}_A^{(1)} - 2k_x\overleftrightarrow{\sigma}_H^{(2)}\right)\cdot\frac{\partial \vec{\varepsilon}}{\partial x} - \frac{\partial \vec{\varepsilon}^{\dagger}}{\partial x}\cdot\overleftrightarrow{\sigma}^{(2)}\cdot\frac{\partial \vec{\varepsilon}}{\partial x}\right\}\end{aligned} \tag{23}$$

If we define

$$\overleftrightarrow{\sigma} \equiv \overleftrightarrow{\sigma}^{(0)} + ik_x\overleftrightarrow{\sigma}^{(1)} - k_x^2\overleftrightarrow{\sigma}^{(2)} \tag{24}$$

then

$$-i\frac{\partial \overleftrightarrow{\sigma}}{\partial k_x} = \overleftrightarrow{\sigma}^{(1)} + 2ik_x\overleftrightarrow{\sigma}^{(2)}$$

and we can write (23) as

$$\vec{J}_x = \left[\overleftrightarrow{\sigma}\cdot\vec{\varepsilon} - i\frac{\partial\overleftrightarrow{\sigma}}{\partial k_x}\cdot\frac{\partial\vec{\varepsilon}}{\partial x} + \overleftrightarrow{\sigma}^{(2)}\cdot\frac{\partial^2\vec{\varepsilon}}{\partial x^2}\right]e^{ik_x x}$$

$$Q_x = \sum_s \frac{1}{2}\mathrm{Re}\left\{\vec{\varepsilon}^\dagger\cdot\left[\frac{-i}{2}\frac{\partial\overleftrightarrow{\sigma}_A}{\partial k_x}\right]\cdot\vec{\varepsilon} + \vec{\varepsilon}^\dagger\cdot\overleftrightarrow{\sigma}^{(2)}\cdot\frac{\partial\vec{\varepsilon}}{\partial x}\right\} \tag{25}$$

$$P_s = \frac{1}{2}\mathrm{Re}\left\{\vec{\varepsilon}^\dagger\cdot\overleftrightarrow{\sigma}_H\cdot\vec{\varepsilon} + \vec{\varepsilon}^\dagger\cdot\left[\overleftrightarrow{\sigma}_A^{(1)} - 2k_x\overleftrightarrow{\sigma}_H^{(2)}\right]\cdot\frac{\partial\vec{\varepsilon}}{\partial x} - \frac{\partial\vec{\varepsilon}^\dagger}{\partial x}\cdot\overleftrightarrow{\sigma}^{(2)}\cdot\frac{\partial\vec{\varepsilon}}{\partial x}\right\}$$

In the weakly damped limit when $\epsilon(x)$ is given by

$$\vec{\varepsilon}(x) = \hat{\varepsilon}e^{-\mathrm{K}x}$$
$$\frac{\partial\vec{\varepsilon}}{\partial x} = -\mathrm{K}\,\vec{\varepsilon} \tag{26}$$

then

$$\mathrm{Re}\left\{\vec{\varepsilon}^\dagger\cdot\overleftrightarrow{\sigma}_A^{(2)}\cdot\frac{\partial\vec{\varepsilon}}{\partial x}\right\} = -\mathrm{K}\;\mathrm{Re}\left\{\vec{\varepsilon}^*\cdot\overleftrightarrow{\sigma}_A^{(2)}\cdot\vec{\varepsilon}\right\} = 0$$

$$\mathrm{Re}\left\{\vec{\varepsilon}^\dagger\cdot\left[-i\frac{\partial\overleftrightarrow{\sigma}_H}{\partial k_x}\right]\cdot\frac{\partial\vec{\varepsilon}}{\partial x}\right\} = -\mathrm{K}\;\mathrm{Re}\left\{\vec{\varepsilon}^\dagger\cdot\left[-i\frac{\partial\overleftrightarrow{\sigma}}{\partial k_x}\right]_A\cdot\vec{\varepsilon}\right\} = 0$$

and (25) reduces to

$$Q_x = \sum_s \frac{1}{2}\mathrm{Re}\left\{\vec{\varepsilon}^\dagger\cdot\left[\frac{-i}{2}\frac{\partial\overleftrightarrow{\sigma}_A}{\partial k_x}\right]\cdot\vec{\varepsilon} - \mathrm{K}\;\vec{\varepsilon}^\dagger\cdot\overleftrightarrow{\sigma}_H^{(2)}\cdot\vec{\varepsilon}\right\}$$
$$P_s = \frac{1}{2}\mathrm{Re}\left\{\vec{\varepsilon}^\dagger\cdot\overleftrightarrow{\sigma}_H\cdot\vec{\varepsilon} - \mathrm{K}^2\;\varepsilon^\dagger\cdot\overleftrightarrow{\sigma}_H^{(2)}\cdot\vec{\varepsilon} + \mathrm{K}\;\vec{\varepsilon}^\dagger\cdot 2k_x\overleftrightarrow{\sigma}_H^{(2)}\cdot\vec{\epsilon}^{(2)}\right\} \tag{27}$$

This agrees with the weak damping WKB result of Bers (Eqs IIA-16,17 in Ref. [18]) when K is small and $\overleftrightarrow{\sigma}_H$ is small (weak damping):

$$Q = \frac{1}{2}\vec{\varepsilon}^\dagger\cdot\left[\frac{-i}{2}\frac{\partial\overleftrightarrow{\sigma}_A}{\partial k_x}\right]\cdot\vec{\varepsilon}$$
$$P = \frac{1}{2}\vec{\varepsilon}^\dagger\cdot\overleftrightarrow{\sigma}_H\cdot\vec{\varepsilon}$$

Thus, we have shown that Eq. (17) is consistent with the WKB result in the weak damping limit for a single wave. But our solutions do not necessarily consist of only a single wave. Instead we have, for example, both fast and Bernstein waves with reflections of each present simultaneously. Therefore, Eq. (17) is most likely not the complete kinetic flux.

4. NUMERICAL RESULTS — COMPLETE SIXTH-ORDER PDE

In this section, we present numerical solutions to the full sixth-order PDE given by Eqs (8) and (9). Figure 1(a) shows schematically the perpendicularly stratified 1-D geometry considered. A plasma slab of width $2a_p$ is located between two perfectly conducting metal walls at $x = \pm x_{\max}$. There is edge plasma in the region $a_p < |x| < |x_{\max}|$. The dashed line represents a current-carrying antenna located in the edge plasma at $x = x_{\text{ant}}$. Figure 1(b) shows the assumed profiles for plasma density $n(x)$, temperatures $T_e(x)$ and $T_i(x)$, and applied magnetic field $B(x)$. These have been chosen to correspond approximately to values along a chord through the

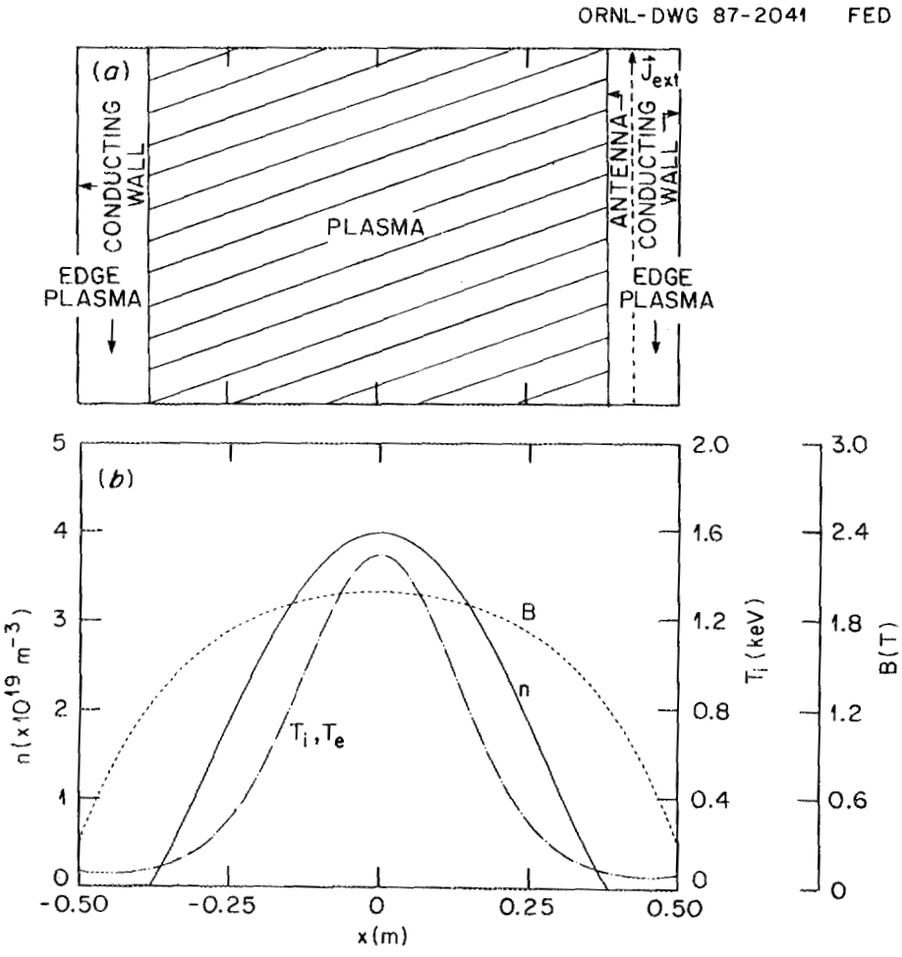

FIG. 1. (a) Perpendicularly stratified 1-D geometry for two-point boundary value problem. (b) Assumed profiles for plasma density, temperature, and applied magnetic field.

axis of the Advanced Toroidal Facility (ATF) stellarator starting from the low-field side, passing through the elliptic plasma, and ending at the opposite low-field side. The profiles are approximately parabolic in x. As with slab model calculations in tokamaks, the poloidal magnetic field and variations of $k_{\|}$ and $v_{\|}$ along $\vec{B}$ are not properly modelled. However, the effect of double minor cyclotron resonance layers and double mode conversion layers in torsatron geometry can be studied. Central plasma parameters and antenna location for the numerical calculations are chosen to be typical of the ATF plasma:

$$R_T = 2.1 \text{ m}$$

$$B_0 = 2 \text{ T}$$

$$a_p = 38 \text{ cm};\ x_{\text{ant}} = 40 \text{ cm};\ x_{\max} = 50 \text{ cm}$$

$$f = \frac{2\pi}{\omega} \sim 30 \text{ MHz}$$

$$n_{e0} \sim 4 \times 10^{13} \text{ cm}^{-3}$$

$$T_{e0} = T_{\text{H}}^0 = T_{\text{D}}^0 = 1500 \text{ eV}$$

$$k_z = 13 \text{ m}^{-1} \qquad \left(n_{\text{toroidal}} = k_z R_T \sim 27\right)$$

$$k_y = 0$$

$$\eta = \frac{n_{\text{H}}}{n_{\text{D}}} = 0.05$$

The finite difference grid consists of 2000–5000 mesh points in the region $-x_{\max} \leq x \leq x_{\max}$.

Figure 2 shows the electric field components E_x, E_y, and E_z for $f = 27$ MHz. Figure 3 shows total energy flux ($S_x = S_{px} + Q_x$), power absorbed by electrons (P_e), minority hydrogen (P_{H}), and majority deuterium (P_{D}) for $f = 27$, 28.4, and 30 MHz. Power is incident from the fast wave generated by the antenna on the right and is partially absorbed and partially reflected at the first pair of resonance layers. Some power is mode converted at the hybrid layer to an ion Bernstein wave which is propagating in the region between the hybrid resonance layers. This is the short-wavelength mode evident in E_x in Fig. 2. At the second pair of resonances, there is more absorption, and the Bernstein wave is reflected from the hybrid layer, allowing the possibility of a standing wave between the two mode conversion layers. Strongly evanescent Bernstein waves in the low-field regions do not grow exponentially as in shooting methods [11].

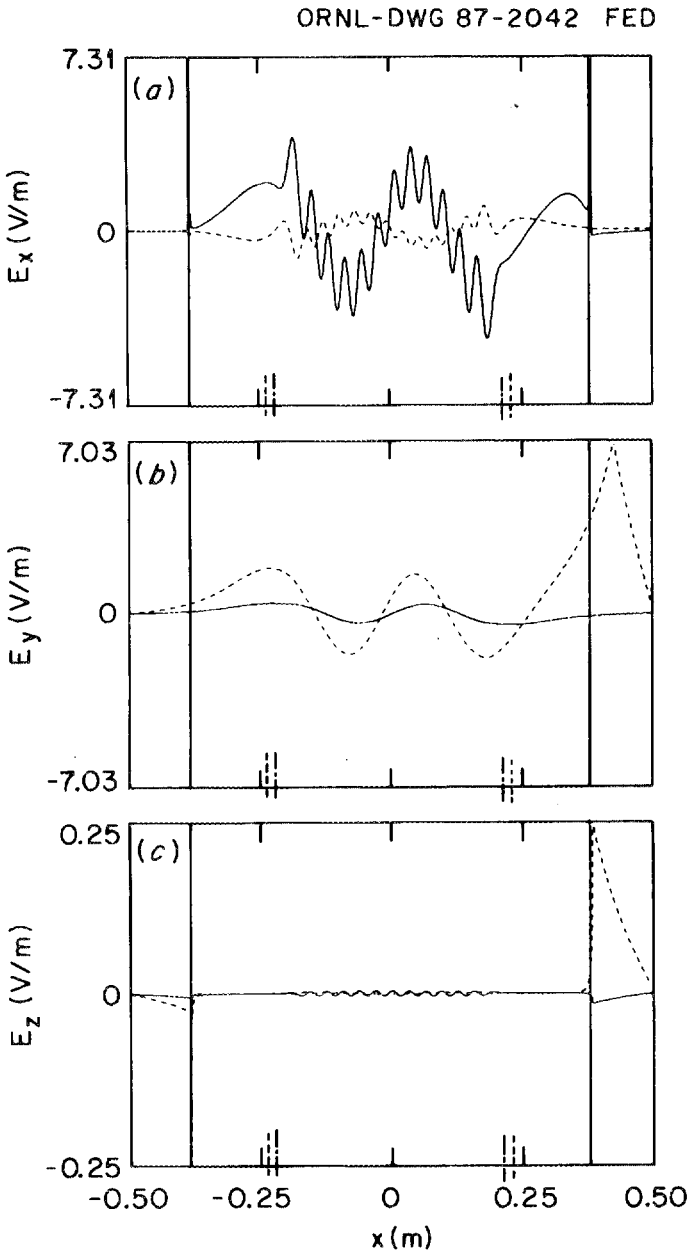

FIG. 2. Real (solid) and imaginary (dashed) parts of (a) E_x, (b) E_y, and (c) E_z for the case of Fig. 1(a).

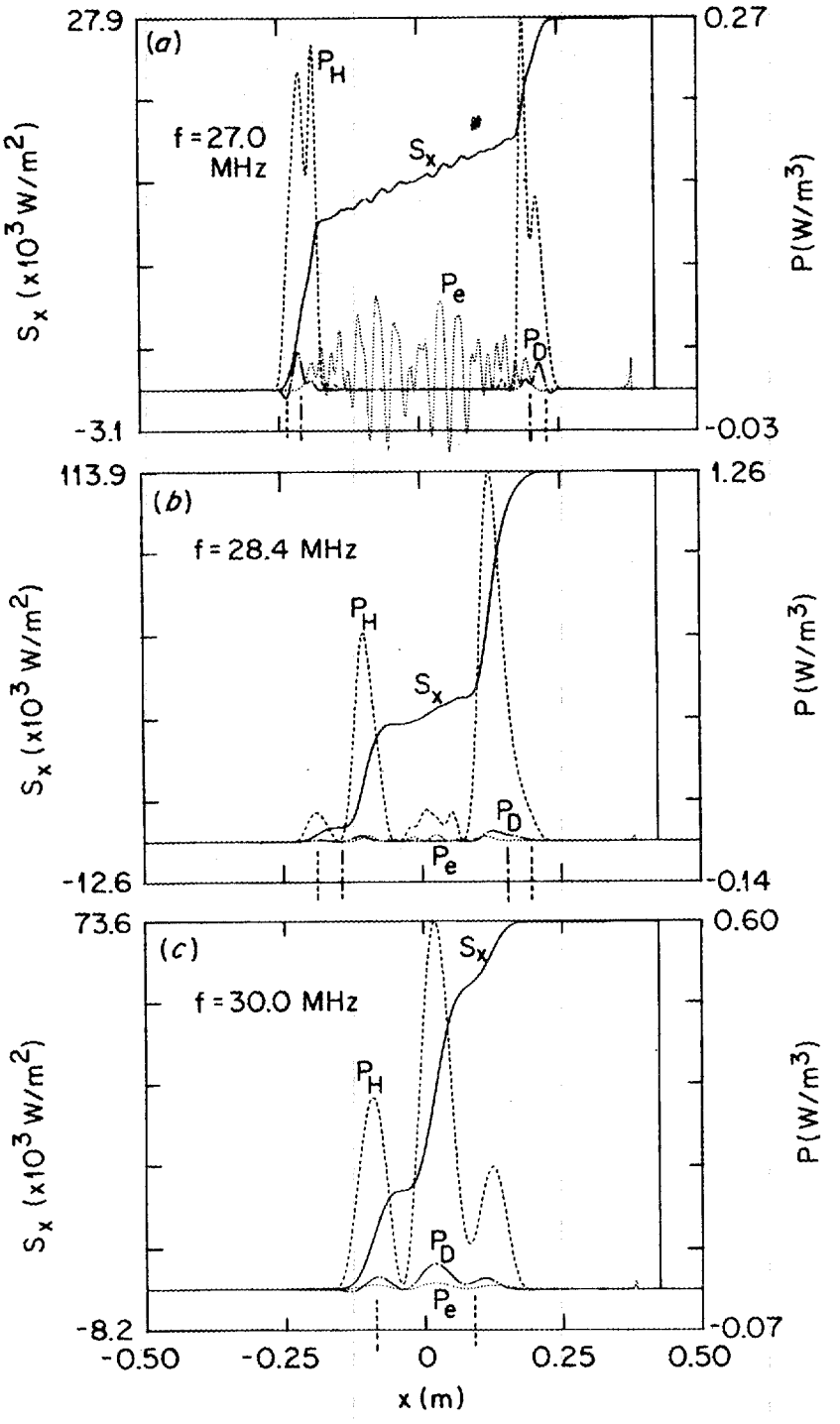

FIG. 3. Total energy flux (S_x) and power absorbed by electrons (P_e), minority hydrogen (P_H), and majority deuterium (P_D) for (a) $f = 27$ MHz, (b) $f = 28.4$ MHz, and (c) $f = 30.0$ MHz.

As the frequency is increased to 28.4 MHz and 30 MHz in Fig. 3, the separation between resonance regions decreases and the mode conversion layers are eventually annihilated at 30 MHz, leaving only the minority cyclotron resonance. The Bernstein wave becomes less evident at 28.4 MHz and disappears entirely at 30 MHz. The non-positive-definite values for P_e in Fig. 3(a) are due to the incomplete choice for Q_x in Eq. (17).

In Fig. 4, we consider a case analogous to that in Figs 2 and 3, but for a tokamak-type magnetic field,

$$B = \frac{B_0}{1 + x/R_T}$$

to compare the results with more conventional shooting calculations [11]. We show reflection, transmission, mode conversion, and absorption coefficients for a 5% minority hydrogen case in the Princeton Large Torus (PLT) tokamak with uniform density and temperature profiles, with

$$R_0 = 1.3 \text{ m}$$

$$B_0 = 3 \text{ T}$$

$$T_e = T_D = T_H = 2000 \text{ eV} = \text{constant}$$

$$n_H = 1.50 \times 10^{12} \text{ cm}^{-3} = \text{constant}$$

$$n_D = 2.85 \times 10^{12} \text{ cm}^{-3} = \text{constant}$$

$$k_z = 1 \text{ to } 10 \text{ m}^{-1}$$

$$k_y = 0$$

The frequency is chosen such that the minority cyclotron resonance occurs at $x = 0$:

$$f = 45.75 \text{ MHz} \left(2\pi f = \Omega_{cH} = \frac{eB_0}{m_H} \text{ at } x = 0 \right)$$

A single fast-wave mode is incident upon the resonance region ($x = 0$) from either the high ($x < 0$) or the low ($x > 0$) magnetic field side. Since the shooting calculations do not include reflected waves but match onto WKB plane wave solutions at the boundaries, we add a strong artificial absorber at the plasma edge ($x \leq 40$ cm) to make the comparison in Fig. 4. The magnitude of the absorption is chosen so that the reflected waves are reduced by about three orders of magnitude. The solutions are then decomposed into incoming and outgoing fast and Bernstein waves to obtain the coefficients shown in Fig. 4.

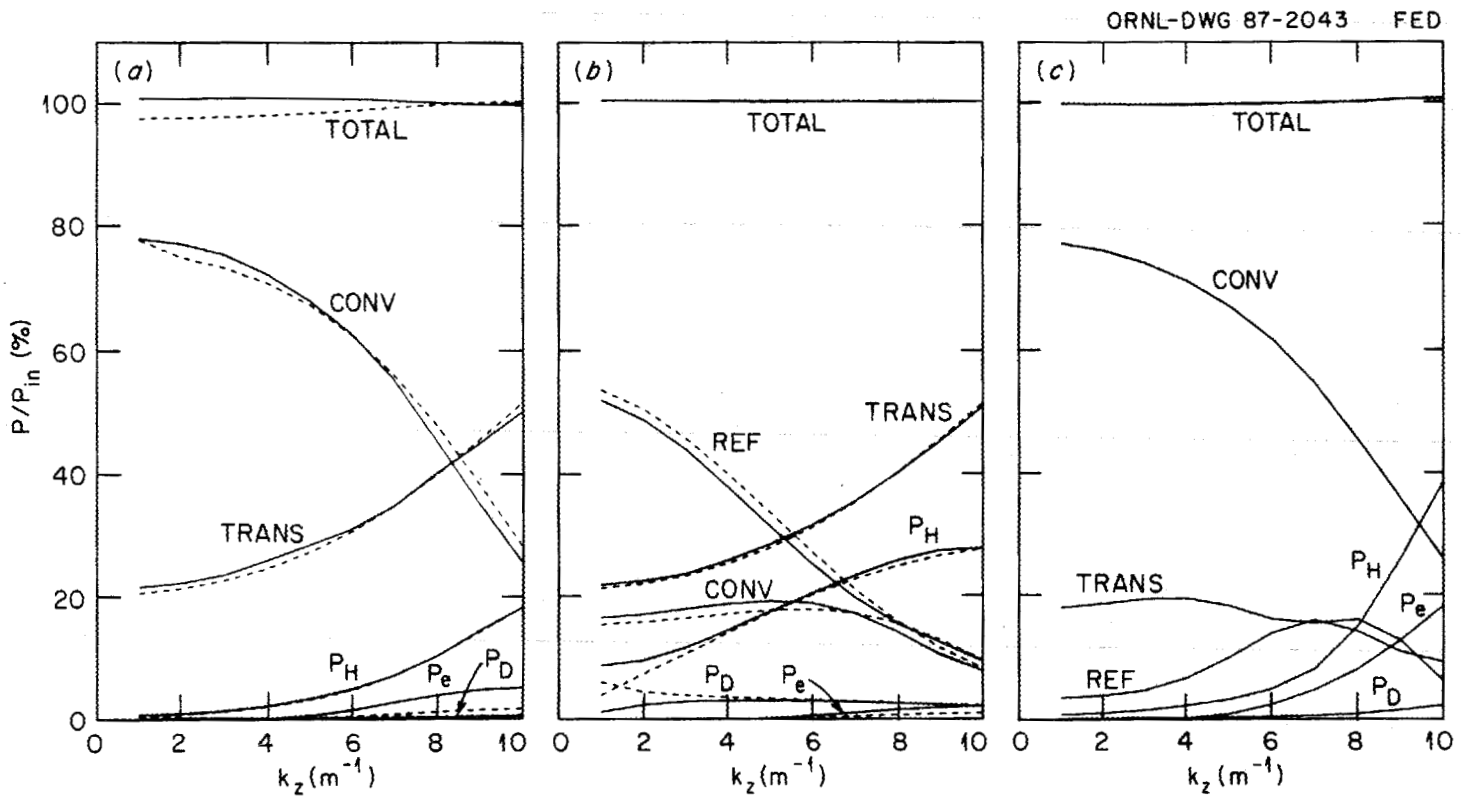

FIG. 4. Comparison to shooting calculations for a tokamak magnetic field for both (a) low and (b) high field incidence. Solid curves show reflection, transmission, mode conversion, and absorption coefficients in PLT for the two-point boundary value calculation; dashed curves show results of a shooting code [11].

Absorption is shown as the percentage of the incoming power absorbed by each species (H, D, e) for low-field incidence and for high-field incidence when k_z is varied from 1 to 10 m^{-1}. Dashed curves show results of the shooting code [11].

In Fig. 5 we illustrate the effect of including the reflected waves and the resulting cavity resonances for the PLT case of Fig. 4. In Fig. 5, the artificial absorber has been removed and replaced with real plasma boundaries, as shown in Fig. 1(a). The edge plasma boundary is at $a_p = \pm 40$ cm, and the conducting wall is at $x_{max} = \pm 50$ cm. The edge plasma density is 1×10^{12} cm^{-3} with $T_e = T_i = 0$ eV. The antenna is placed in the edge plasma region and at $x = 43$ cm for low-field incidence and at $x = -43$ cm for high-field incidence. Note that the variations of the reflection, transmission, and conversion coefficients are no longer smooth as in Fig. 4 but now show strong peaks and valleys at particular values of k_z. These peaks and valleys are caused by cavity modes in which the reflected Bernstein waves coming back from the wall convert to fast waves, which either add to or subtract from the transmitted fast waves. As the reflected ion Bernstein wave disappears at large k_z due to Landau damping, this interference effect also disappears. At the peaks, the values of the transmission and conversion coefficients (as defined in Fig. 4) can be greater than 100%. But there are two additional transmission and conversion coefficients shown by the dashed curves in Fig. 5 (rtrans and rconv) which are very nearly equal and opposite in sign to the standard definitions. These are defined using the reflections of the transmitted and converted waves, respectively. Thus, the total of all the coefficients is still 100%, as it must be to conserve energy. A comparison of Figs 4 and 5 shows the importance of including plasma boundaries if meaningful comparisons with experiment are to be made.

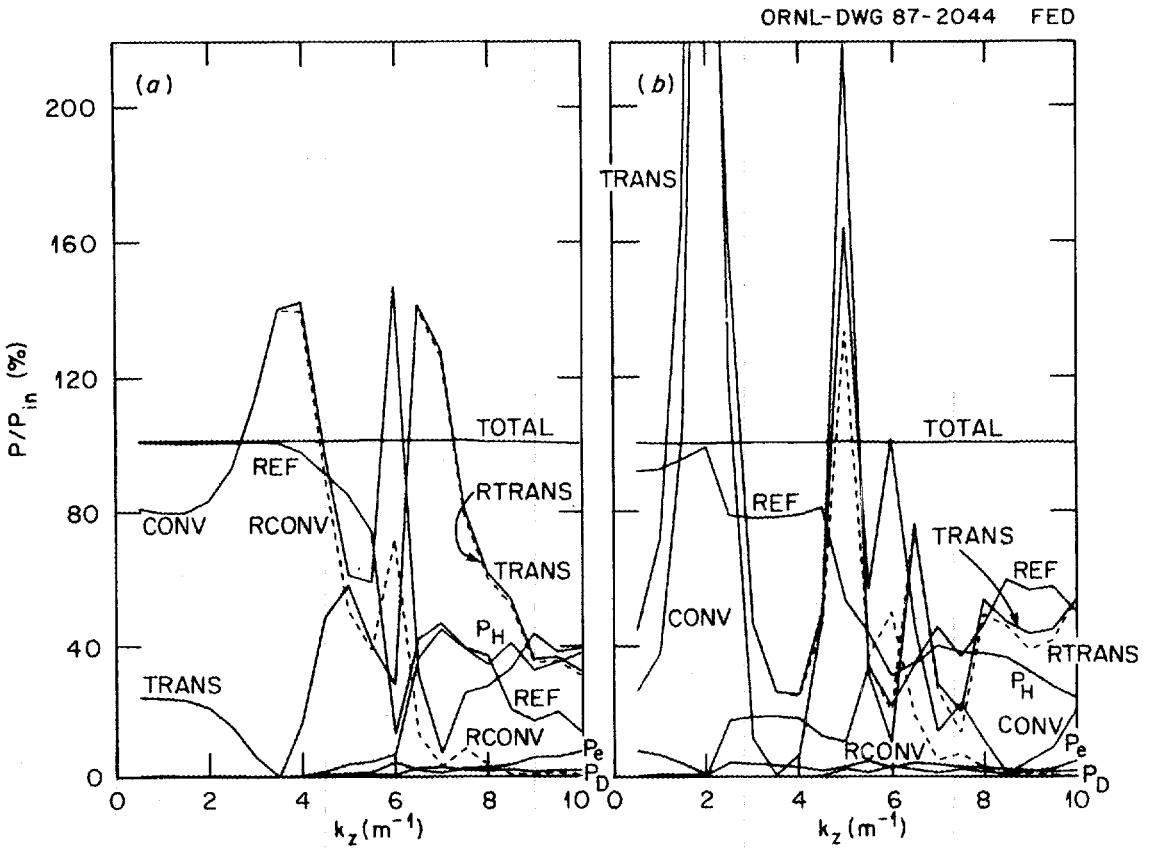

FIG. 5. Effect of including reflected waves and the resulting cavity modes on the result of Fig. 4.

5. APPROXIMATE WAVE EQUATION USING LOCAL DISPERSION THEORY

A local dispersion relation can be found by assuming $\vec{E}(x) \sim \vec{E}\exp(ik_x x)$ in the wave equation so that $\partial\vec{E}/\partial x \rightarrow ik_x\vec{E}$. In the absence of a driving current, Eq. (8) gives

$$\left(\vec{n}\cdot\vec{E}\right)\vec{n} - |n|^2\vec{E} + \left(\overleftrightarrow{\epsilon}^{(0)} + \overleftrightarrow{\delta}^{(1)} + \overleftrightarrow{\zeta}^{(2)}\right)\cdot\vec{E} + ik_x\left(\overleftrightarrow{\epsilon}^{(1)} + \overleftrightarrow{\delta}^{(2)}\right)_U\cdot\vec{E} + \vec{E}\cdot\frac{\partial}{\partial x}\left(\overleftrightarrow{\epsilon}^{(1)} + \overleftrightarrow{\delta}^{(2)}\right)_L + ik_x\left(\overleftrightarrow{\epsilon}^{(1)} + \overleftrightarrow{\delta}^{(2)}\right)_L\cdot\vec{E} + ik_x\frac{\partial\overleftrightarrow{\epsilon}^{(2)}}{\partial x}\cdot\vec{E} - k_x^2\overleftrightarrow{\epsilon}^{(2)}\cdot\vec{E} = 0 \tag{28}$$

A nonzero solution for $\vec{E}$ in Eq. (28) requires

$$\det\left[\vec{n}\vec{n} - |n|^2\overleftrightarrow{I} + \left(\overleftrightarrow{\epsilon}^{(0)} + \overleftrightarrow{\delta}^{(1)} + \overleftrightarrow{\zeta}^{(2)}\right) + \frac{\partial}{\partial x}\left(\overleftrightarrow{\epsilon}^{(1)} + \overleftrightarrow{\delta}^{(2)}\right)_L + k_x\left(i\left[\overleftrightarrow{\epsilon}^{(1)} + \overleftrightarrow{\delta}^{(2)}\right]_U + i\left[\overleftrightarrow{\epsilon}^{(1)} + \overleftrightarrow{\delta}^{(2)}\right]_L + i\frac{\partial\overleftrightarrow{\epsilon}^{(2)}}{\partial x}\right) + k_x^2\left(-\overleftrightarrow{\epsilon}^{(2)}\right)\right] = 0 \tag{29}$$

where $\vec{n} = \vec{k}/k_0$. In the plasma, Eq. (29) is sixth order in k_x, and in the vacuum it is fourth order. Figure 6(a) shows all six roots for $n_\perp^2 \equiv (k_x/k_0)^2$ as functions of x for the case of Fig. 3(b) (28.4 MHz). Figure 6(b) shows only the root corresponding to the fast wave travelling in the $-\hat{x}$ direction.

As suggested in Refs [14,15], an approximate second-order wave equation to treat only the fast wave can be constructed by replacing $\vec{E}$ by $\vec{E}\exp(ik_x x)$ in just the warm plasma terms in Eq. (8). This leads to

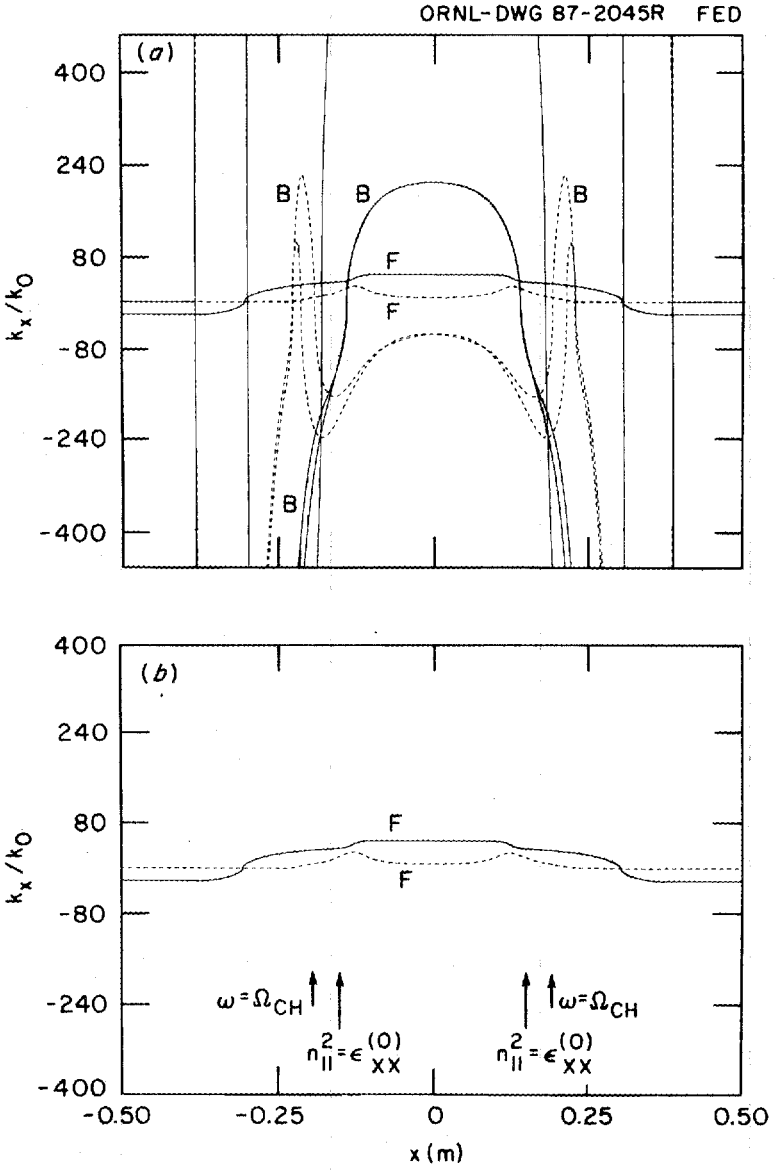

FIG. 6. (a) All six roots to the local dispersion relation [Eq. (29)] for the case of Fig. 2(b) (f = 28.4 MHz). (b) Only the root corresponding to the fast wave travelling in the $-\hat{x}$ direction.

$$-\frac{1}{k_0^2}\left(\nabla\times\nabla\times\vec{E}\right)+\left\{\left(\overleftrightarrow{\epsilon}^{(0)}+\overleftrightarrow{\delta}^{(1)}+\overleftrightarrow{\zeta}^{(2)}+\frac{\partial}{\partial x}\left[\overleftrightarrow{\epsilon}^{(1)}+\overleftrightarrow{\delta}^{(2)}\right]_L\right)+k_x\left(i\left[\overleftrightarrow{\epsilon}^{(1)}+\overleftrightarrow{\delta}^{(2)}\right]_U+i\left[\overleftrightarrow{\epsilon}^{(1)}+\overleftrightarrow{\delta}^{(2)}\right]_L+i\frac{\partial\overleftrightarrow{\epsilon}^{(2)}}{\partial x}\right)+k_x^2\left(-\overleftrightarrow{\epsilon}^{(2)}\right)\right\}\cdot\vec{E}=\frac{-i}{\omega\epsilon_0}\vec{J}_{\text{ext}} \tag{30}$$

where k_x is taken to be the root of the dispersion relation, Eq. (29), corresponding to the fast wave [i.e. Fig. (6b)]. The $\hat{x}$, $\hat{y}$, and $\hat{z}$ components of Eq. (30) are

$$\begin{aligned}
&\left[\left(\epsilon_{xx}^{(0)}+\zeta_{xx}^{(2)}-n_y^2-n_z^2\right)+k_x\left(i\frac{\partial\epsilon_{xx}^{(2)}}{\partial x}\right)+k_x^2\left(-\epsilon_{xx}^{(2)}\right)\right]E_x-\frac{in_y}{k_0}\frac{\partial E_y}{\partial x}\\
&\quad+\left[\left(\epsilon_{xy}^{(0)}+\zeta_{xy}^{(2)}\right)+k_x\left(i\delta_{xy}^{(2)}+i\frac{\partial\epsilon_{xy}^{(2)}}{\partial x}\right)+k_x^2\left(-\epsilon_{xy}^{(2)}\right)\right]E_y\\
&\quad-\frac{in_z}{k_0}\frac{\partial E_z}{\partial x}+\left[\delta_{xz}^{(1)}+k_x\left(i\epsilon_{xz}^{(1)}\right)\right]E_z=\frac{-i}{\omega\epsilon_0}J_{\text{ext},x}\\
&-\frac{in_y}{k_0}\frac{\partial E_x}{\partial x}+\left[\left(\epsilon_{yx}^{(0)}+\zeta_{yx}^{(2)}+\frac{\partial\delta_{yx}^{(2)}}{\partial x}\right)+k_x\left(i\delta_{yx}^{(2)}+i\frac{\partial\epsilon_{yx}^{(2)}}{\partial x}\right)\right.\\
&\quad\left.+k_x^2\left(-\epsilon_{yx}^{(2)}\right)\right]E_x+\frac{1}{k_0^2}\frac{\partial^2E_y}{\partial x^2}+\left[\left(\epsilon_{yy}^{(0)}+\zeta_{yy}^{(2)}-n_z^2\right)\right.\\
&\quad\left.+k_x\left(i\frac{\partial\epsilon_{yy}^{(2)}}{\partial x}\right)+k_x^2\left(-\epsilon_{yy}^{(2)}\right)\right]E_y+\left[\left(\delta_{yz}^{(1)}+n_yn_z\right)\right.\\
&\quad\left.+k_x\left(i\epsilon_{yz}^{(1)}\right)\right]E_z=\frac{-i}{\omega\epsilon_0}J_{\text{ext},y}\\
&-\frac{in_z}{k_0}\frac{\partial E_x}{\partial x}+\left[\frac{\partial\epsilon_{zx}^{(1)}}{\partial x}+\delta_{zx}^{(1)}+k_x\left(i\epsilon_{zx}^{(1)}\right)\right]E_x+\left[\left(n_yn_z+\delta_{zy}^{(1)}+\frac{\partial\epsilon_{zy}^{(1)}}{\partial x}\right)\right.\\
&\quad\left.+k_x\left(i\epsilon_{zy}^{(1)}\right)\right]E_y+\frac{1}{k_0^2}\frac{\partial^2E_z}{\partial x^2}+\left[\left(\epsilon_{zz}^{(0)}+\zeta_{zz}^{(2)}-n_y^2\right)\right.\\
&\quad\left.+k_z\left(i\frac{\partial\epsilon_{zz}^{(2)}}{\partial x}\right)+k_z^2\left(-\epsilon_{zz}^{(2)}\right)\right]E_z=\frac{-i}{\omega\epsilon_0}J_{\text{ext},z}
\end{aligned} \tag{31}$$

6. NUMERICAL RESULTS — APPROXIMATE SECOND-ORDER PDE

In this section, we present numerical solutions of the approximate PDE given by Eqs (30) and (31). By comparing to solutions of the complete sixth-order equation in Section 4, we can evaluate the usefulness of the approximate equation in the more complicated 2-D geometry.

In Fig. 7 we compare the approximate second-order solution and the complete sixth-order solution for the low-field incidence, tokamak calculation in Fig. 4. There

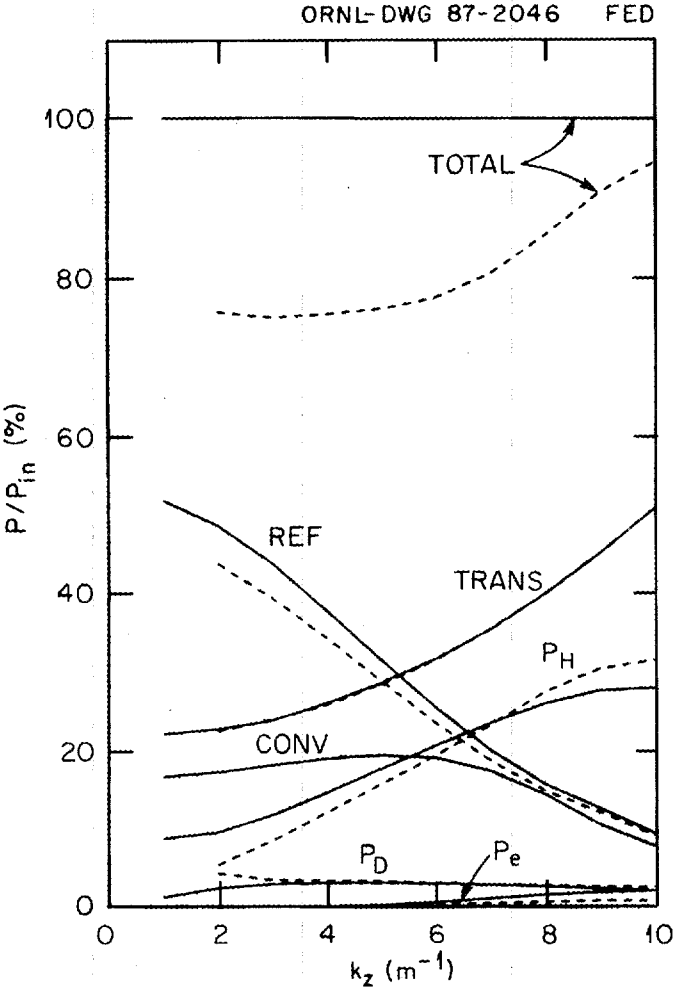

FIG. 7. Comparison between approximate second-order (dashed) and complete sixth-order (solid) global coefficients for low-field incidence in PLT.

is reasonable agreement for all coefficients except mode conversion, which is obviously not included in the second-order equation and accounts for the energy decrement in the approximate result. A similar comparison for high-field incidence was not possible since the fast wave root to the dispersion relation was not continuous for $k_z \lesssim 9\ \mathrm{m}^{-1}$. In this case, the fast wave incident from the high-field side connects continuously onto the Bernstein wave branch.

In Fig. 8 we compare profiles for energy flux and power absorbed at $k_z = 10\ \mathrm{m}^{-1}$ for the low-field incidence case in Fig. 7. We see that although the global transmission, reflection, and absorption coefficients in Fig. 7 agree fairly well, the detailed shapes of the power absorption profiles in Fig. 8 are not very similar. Since reflections have been eliminated from this calculation, the differences seen in Fig. 8 cannot be due to the presence of reflected waves. The main deficiency in the approximate second-order equation is the inability to distinguish between power absorbed and power converted to the Bernstein wave. For example, the strong peaking in the power absorbed by minority hydrogen, P_{H}, in Fig. 8(b) occurs at $x \simeq -5$ cm, which is very nearly the location of the mode conversion surface. This peaking in P_{H} is actually the power that is mode converted in the complete sixth-order solution of Fig. 8(a).

In Fig. 9 we compare the exact warm plasma solution of Fig. 2(b) ($f = 28.4$ MHz) with an approximate second-order calculation and with a cold plasma calculation from Eq. (8) with $T_{\mathrm{e}} = T_{\mathrm{i}} = 0$ and ad hoc collisions [1–5] $(\nu/\omega = 10^{-2})$ to broaden the minority cyclotron resonance. The approximate second-order calculation is significantly better in this case than the cold plasma calculation with ad hoc collisions. The agreement here might be expected, since the Bernstein wave is not fully developed due to the proximity of the two mode conversion layers, and the neglect of details of the Bernstein wave inherent in Eq. (30) is not expected to cause a significant problem. On the other hand, in Fig. 10 ($f = 27.5$ MHz) the Bernstein wave appears to be fully developed and the approximate second-order equation gives a noticeably different result from the complete sixth-order equation, but it probably still gives a more accurate result than the cold plasma calculation with ad hoc collisions.

Although the discrepancy in Fig. 10 appears large, it can be argued that our neglect of variations of $k_{||}$ and $v_{||}$ along $\vec{B}$ has led to artificially weak damping of the Bernstein wave. In experiments, for example, very strong damping of the Bernstein wave is observed outside the immediate vicinity of the resonance and mode

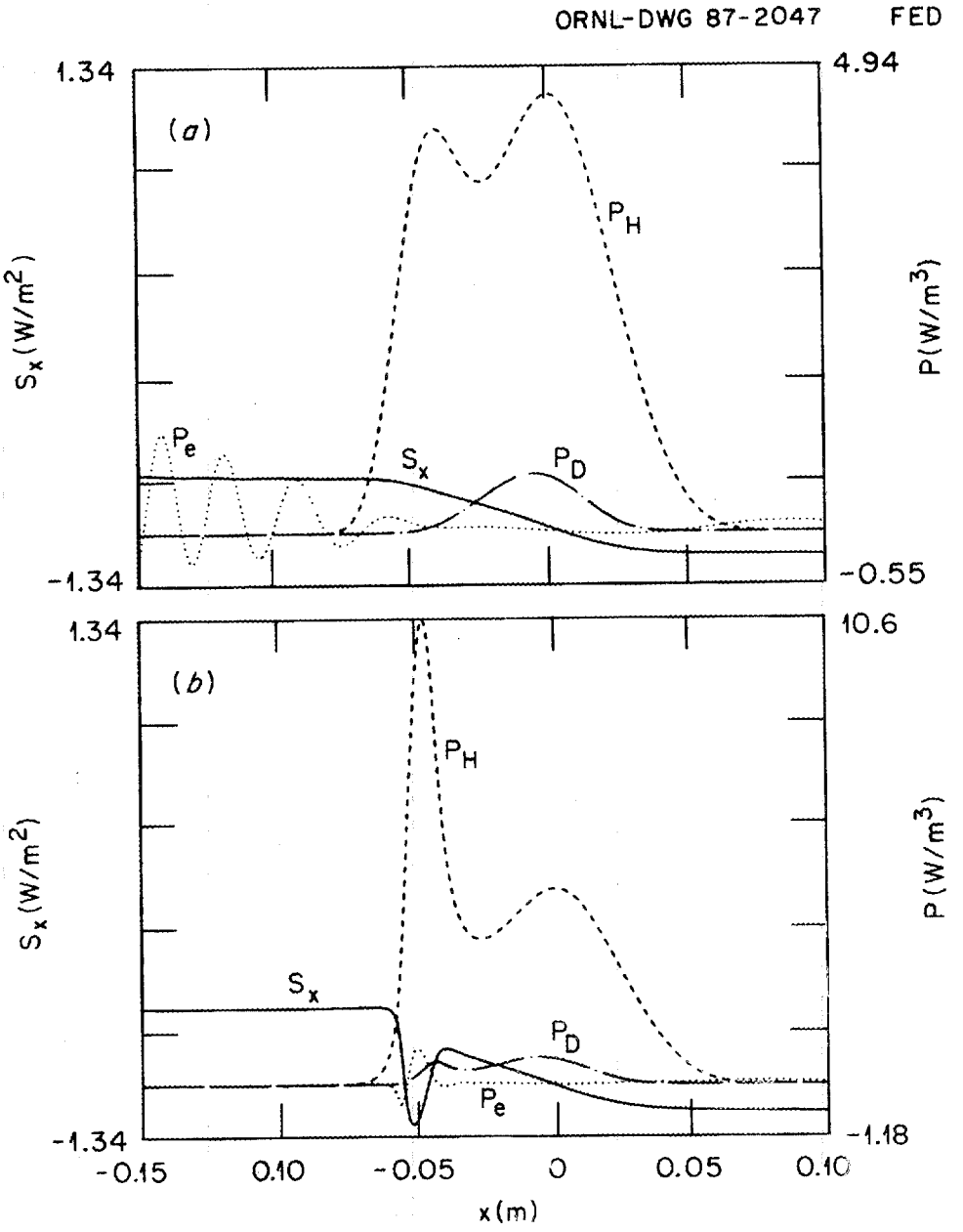

FIG. 8. Comparison between (a) complete and (b) approximate energy flux and power deposition profiles in PLT with $k_z = 10$ m^{-1} and low-field incidence.

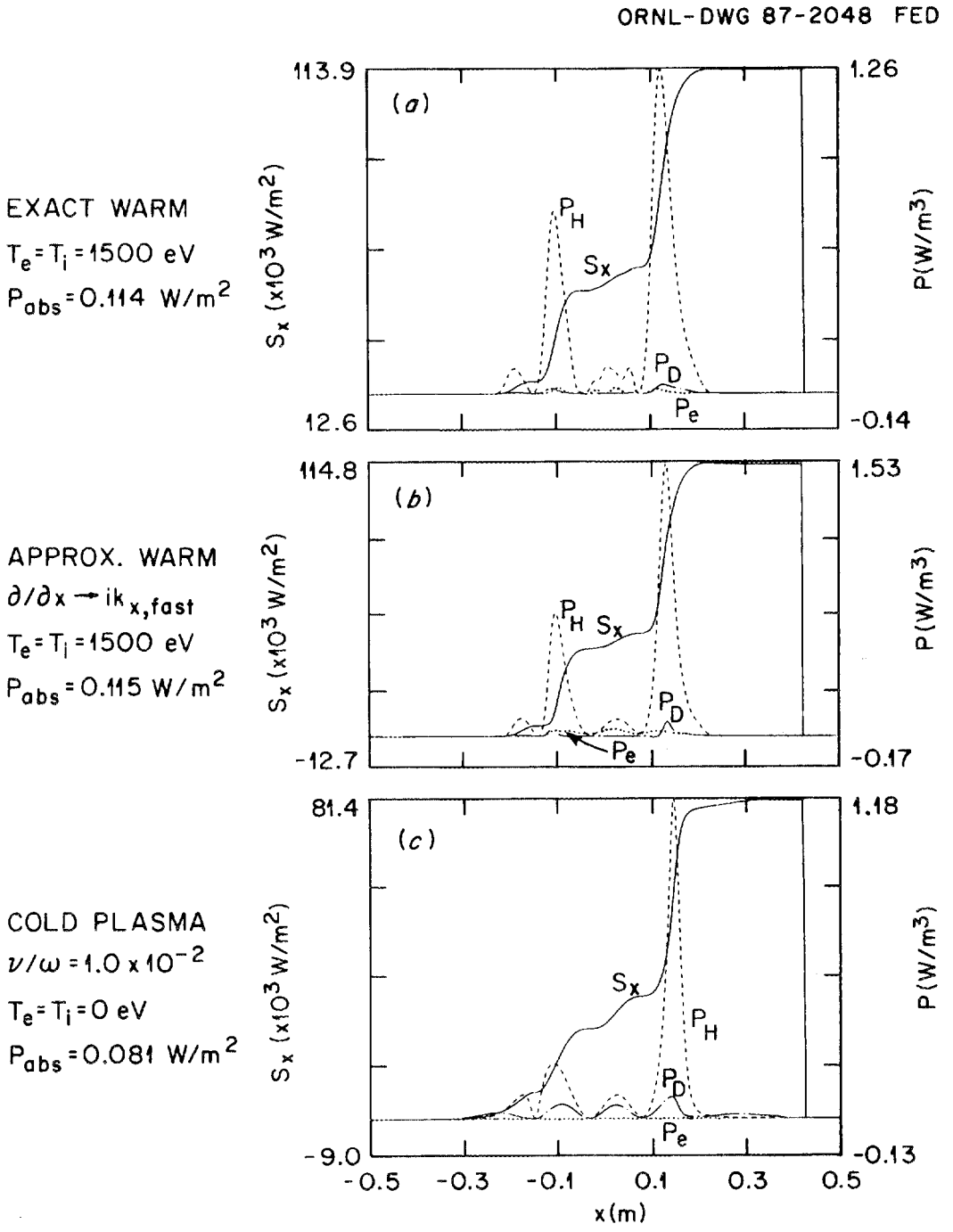

FIG. 9. Comparison of exact warm, approximate warm, and cold plasma calculations for the ATF case in Fig. 2(b) ($f = 28.4$ MHz and $k_z = 13.0$ m^{-1}).

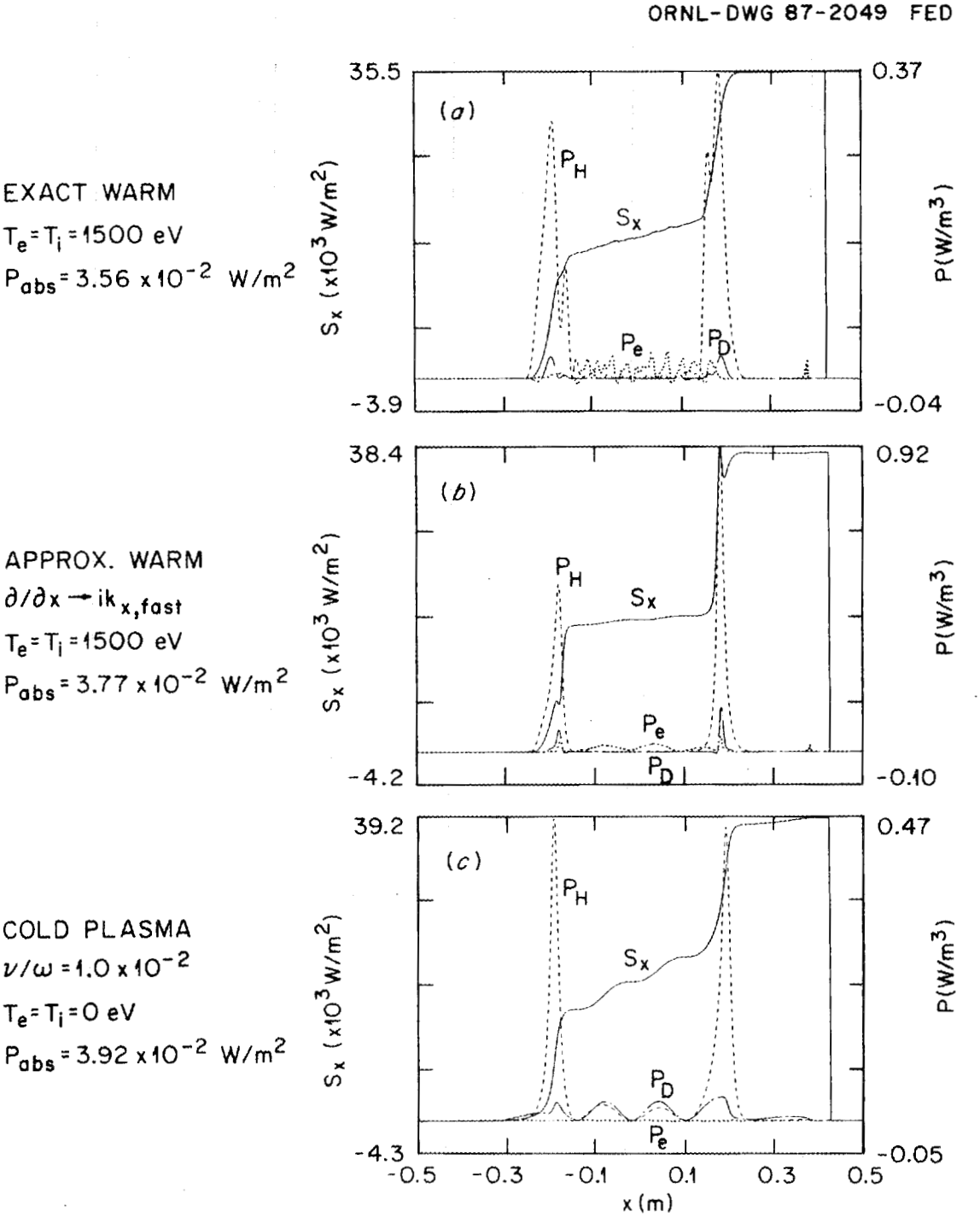

FIG. 10. Comparison of exact warm, approximate warm, and cold plasma calculations for ATF with $f = 27.5$ MHz and $k_z = 13.0$ m^{-1}.

conversion layers [19]. Damping of the Bernstein wave can be artificially enhanced in our calculation by adding a small real part to the second-order conductivity [10]. Thus we add $-\delta(\epsilon_0\omega/k_0^2)$ to the diagonals of the second-order conductivity tensor $\overleftrightarrow{\sigma}^{(2)}$ within the plasma where $\delta = 10^{-3}$. Repeating the calculations of Fig. 10 now shows a strongly damped Bernstein wave in the complete solution but no better agreement with the approximate solution. Thus, we conclude that it is not the lack of damping of the Bernstein wave which leads to the poor approximate result in this case.

7. SUMMARY AND CONCLUSIONS

We have shown that the complete sixth-order wave equation can be solved globally as a two-point boundary value problem in a perpendicularly stratified 1-D slab plasma. Furthermore, strongly evanescent Bernstein waves in the low-field regions do not grow exponentially as in shooting methods. Strong variations in the absorption and in the structure of the wave electric fields occur as the resonance topology is varied. Inclusion of ∇p drifts and the associated anisotropy in the equilibrium distribution function results in a self-adjoint system with *no* physical dissipation far from resonance.

Inclusion of the plasma boundaries leads to reflected waves and associated cavity modes that are left out of shooting calculations where WKB plane wave solutions are matched at the boundaries.

An approximate second-order differential equation derived from local dispersion theory gives a good approximation to the full solution of the sixth-order system in some cases when the Bernstein waves are not dominant. While global reflection, transmission, and absorption coefficients agree quite well with the complete solution, the detailed profiles for power deposition are somewhat different. Adding artificial damping in these cases to simulate the experimentally observed strong damping, which results from variations in $k_{||}$ and $v_{||}$ along $\vec{B}$, does not appear to improve the agreement. Future work should include more realistic modelling of the radial and poloidal magnetic fields, including variations of $k_{||}$ and $v_{||}$ along $\vec{B}$.

APPENDIX

In this appendix we derive the warm plasma conductivity tensor following the method of Martin and Vaclavik [13]. The collisionless Boltzmann equation or Vlasov equation,

$$\frac{\partial \tilde{f}}{\partial t} + \vec{v} \cdot \nabla \tilde{f} + \frac{e}{m}\left(\vec{E} + \vec{v} \times \vec{B}\right) \cdot \frac{\partial \tilde{f}}{\partial \vec{v}} = 0 \tag{A.1}$$

can be linearized in the presence of a time-dependent perturbation with

$$\begin{aligned} \tilde{f} &= F(\vec{x}, \vec{v}) + f(\vec{x}, \vec{v}, t) \\ \vec{B} &= B_0(\vec{x}) + \vec{B}(\vec{x}, t) \\ \vec{E} &= \vec{E}(\vec{x}, t) \end{aligned} \tag{A.2}$$

where $f, \vec{B}$, and $\vec{E}$ are assumed small with y, z, and t dependences

$$\left.\begin{matrix} f \\ B \\ E \end{matrix}\right\} \propto \exp[i(k_y y + k_z z - \omega t)] \tag{A.3}$$

The unperturbed quantities are assumed to be functions of x only, and $\vec{B}_0$ is taken in the $\hat{z}$ direction,

$$\begin{aligned} \vec{B}_0 &= B_0(x)\,\hat{z} \\ F &= F(x, \vec{v}) \end{aligned} \tag{A.4}$$

Thus, Eq. (A.1) gives (using $\nabla \times \vec{E} = i\omega \vec{B}$)

$$v_x \frac{\partial F}{\partial x} + \Omega\left(v_y \frac{\partial F}{\partial v_x} - v_x \frac{\partial F}{\partial v_y}\right) = 0 \tag{A.5}$$

and

$$\begin{aligned} -i(\omega - k_z v_z - k_y v_y) f + v_x \frac{\partial f}{\partial x} + \Omega\left(v_y \frac{\partial f}{\partial v_x} - v_x \frac{\partial f}{\partial v_y}\right) \\ = -\frac{e}{m}\left(\vec{E} + \vec{v} \times \frac{1}{i\omega}\left[\nabla \times \vec{E}\right]\right) \cdot \frac{\partial F}{\partial \vec{v}} \end{aligned} \tag{A.6}$$

where $\Omega = eB_0(x)/m$. Now we transform from v_x, v_y, v_z to $v_\perp, \phi, v_\parallel$, where ϕ is the gyroangle, so that

$$\begin{aligned} v_x &= v_\perp \cos\phi \\ v_y &= v_\perp \sin\phi \\ v_z &= v_\parallel \end{aligned} \tag{A.7}$$

Then

$$\frac{\partial}{\partial\phi} = v_x\frac{\partial}{\partial v_y} - v_y\frac{\partial}{\partial v_x}$$

$$E_x v_x + E_y v_y = \frac{v_\perp}{2}\left(E_+ e^{-i\phi} + E_- e^{i\phi}\right)$$

where $E_+ = E_x + iE_y$ and $E_- = E_x - iE_y$. Now Eq. (A.5) can be written

$$\frac{v_\perp \cos\phi}{\Omega}\frac{\partial F}{\partial x} - \frac{\partial F}{\partial\phi} = 0$$

To solve this for F, assume the Larmor radius $\rho = v_\perp/\Omega$ is small compared with the gradient scale length and proceed iteratively. This gives

$$F\left(x, v_\perp, v_\parallel, \phi\right) = F^{(0)}\left(x, v_\perp, v_\parallel\right) + \frac{v_y}{\Omega}\frac{\partial F^{(0)}}{\partial x} + \frac{v_y^2}{2\Omega}\frac{\partial}{\partial x}\left[\frac{1}{\Omega}\frac{\partial F^{(0)}}{\partial x}\right] \qquad \text{(A.8)}$$

Likewise Eq. (A.6) can be written as

$$-i\left(\omega - k_z v_z\right) f + \frac{v_\perp}{2}\left[\left(\frac{\partial f}{\partial x} + k_y f\right)e^{i\phi} + \left(\frac{\partial f}{\partial x} - k_y f\right)e^{-i\phi}\right]$$
$$- \Omega\frac{\partial f}{\partial\phi} = \frac{-e}{m}\left[\vec{E} + \frac{1}{i\omega}\vec{v}\times\left(\nabla\times\vec{E}\right)\right]\cdot\frac{\partial F}{\partial\vec{v}} \qquad \text{(A.9)}$$

To simplify the calculation of $\partial F/\partial\vec{v}$ on the right-hand side, we take $F^{(0)} = F^{(0)}(x, v)$ only; i.e. $F^{(0)}$ is isotropic in $\vec{v}$. Note, however, that the total $F = F(x, v, v_y)$ is not isotropic; thus, the term $\vec{v}\times\nabla\times\vec{E}_1$ on the right-hand side must be included. Now for $F = F(x, v, v_y)$,

$$\frac{\partial F}{\partial\vec{v}} = \frac{\partial F}{\partial v}\hat{v} + \frac{\partial F}{\partial v_y}\hat{y}$$

and using Eq. (A.8) this is

$$\frac{\partial F}{\partial\vec{v}} = \left[G + \frac{v_y}{\Omega}G' + \frac{v_y^2}{2\Omega}\frac{\partial}{\partial x}\left(\frac{G'}{\Omega}\right)\right]\hat{v} + \left[\frac{1}{\Omega}F' + \frac{v_y}{\Omega}\frac{\partial}{\partial x}\left(\frac{F'}{\Omega}\right)\right]\hat{y}$$

where $G = \partial F^{(0)}/\partial v$ and $F' = \partial F^{(0)}/\partial x$. Substituting into the right-hand side of (A.9) (which we define as A) gives

$$A \equiv \frac{-e}{m}\left[\vec{E} + \frac{1}{i\omega}\vec{v}\times\left(\nabla\times\vec{E}\right)\right]\cdot\frac{\partial F}{\partial\vec{v}} = A^{(0)} + A^{(1)} + A^{(2)}$$

where the superscript denotes the order with respect to $\rho = v_\perp/\Omega$ and

$$
\begin{aligned}
A^{(0)} &= \frac{-e}{m}\frac{G}{v}\left\{\frac{v_\perp}{2}\left(E_x\left[e^{-i\phi}+e^{i\phi}\right]+iE_y\left[e^{-i\phi}-e^{i\phi}\right]\right)+E_z v_z\right\} \\
A^{(1)} &= \frac{-e}{m}\left\{\frac{G'v_\perp^2}{4\Omega v}\left(iE_x\left[e^{-2i\phi}-e^{2i\phi}\right]+E_y\left[2-e^{2i\phi}-e^{-2i\phi}\right]\right)\right. \\
&\quad \left.+\frac{G'}{\Omega}\frac{v_\perp}{v}\left(\frac{i}{2}v_z E_z\left[e^{-i\phi}-e^{i\phi}\right]\right)+\frac{F'}{\Omega}E_y\left(1-\frac{k_z v_z}{\omega}\right)\right\} \\
A^{(2)} &= \frac{-e}{m}\left\{\frac{v_\perp^3}{16v\Omega}\frac{\partial}{\partial x}\left(\frac{G'}{\Omega}\right)\left[E_x\left(e^{i\phi}+e^{-i\phi}-e^{-3i\phi}-e^{3i\phi}\right)\right.\right. \\
&\quad \left.+iE_y\left(3e^{-i\phi}-3e^{i\phi}-e^{-3i\phi}+e^{3i\phi}\right)\right] \\
&\quad +\frac{v_\perp^2}{4v\Omega}\frac{\partial}{\partial x}\left(\frac{G'}{\Omega}\right)E_z v_z\left(1-\frac{1}{2}e^{2i\phi}-\frac{1}{2}e^{-2i\phi}\right) \\
&\quad +i\frac{v_\perp}{2\Omega}\frac{\partial}{\partial x}\left(\frac{F'}{\Omega}\right)E_y\left(1-\frac{k_z v_z}{\omega}\right)\left(e^{-i\phi}-e^{i\phi}\right) \\
&\quad \left.+\frac{F'}{\Omega\omega}\left[v_z k_y E_z+\frac{v_\perp}{2}\left(e^{i\phi}+e^{-i\phi}\right)\left(k_y E_x+i\frac{\partial E_y}{\partial x}\right)\right]\right\}
\end{aligned}
\tag{A.10}
$$

Now we Fourier expand f and A in the gyroangle ϕ

$$
\begin{aligned}
f\left(x,v_\perp,v_\parallel,\phi\right) &= \sum_{n=-\infty}^{\infty} f_n\left(x,v_\perp,v_\parallel\right)e^{in\phi} \\
A\left(x,v_\perp,v_\parallel,\phi\right) &= \sum_{n=-\infty}^{\infty} A_n\left(x,v_\perp,v_\parallel\right)e^{in\phi}
\end{aligned}
$$

and the linearized Vlasov equation in (A.9) becomes

$$
\begin{aligned}
&\sum_{n=-\infty}^{\infty} e^{in\phi}\left\{-i\left(\omega-k_z v_z+n\Omega\right)f_n+\frac{v_\perp}{2}\left(L^+e^{i\phi}+L^-e^{-i\phi}\right)f_n\right\} \\
&\qquad = \sum_{n=-\infty}^{\infty}\left(A_n^{(0)}+A_n^{(1)}+A_n^{(2)}\right)e^{in\phi}
\end{aligned}
\tag{A.11}
$$

where $L^+ \equiv \partial/\partial x + k_y$ and $L^- = \partial/\partial x - k_y$. Equating individual coefficients of $e^{in\phi}$ gives

$$
i\Delta_n f_n+\frac{v_\perp}{2}\left(L^+ f_{n-1}+L^- f_{n+1}\right) = A_n^{(0)}+A_n^{(1)}+A_n^{(2)} \tag{A.12}
$$

where we have defined the "resonant denominator" Δ_n to be

$$\Delta_n \equiv -(\omega - k_z v_z + n\Omega) = k_z v_z - (\omega + n\Omega) \tag{A.13}$$

To solve (A.12) assume that $\rho = v_\perp/\Omega$ is small and proceed iteratively. To lowest order in ρ, neglect the $v_\perp$ terms to obtain

$$f_n^{(0)} = \frac{A_n^{(0)}}{i\Delta_n} \tag{A.14}$$

To first order in ρ

$$f_n^{(1)} = \frac{1}{i\Delta_n}\left[A_n^{(1)} - \frac{v_\perp}{2}\left(L^+ f_{n-1}^{(0)} + L^- f_{n+1}^{(0)}\right)\right] \tag{A.15}$$

and to second order in ρ

$$f_n^{(2)} = \frac{1}{i\Delta_n}\left[A_n^{(2)} - \frac{v_\perp}{2}\left(L^+ f_{n-1}^{(1)} + L^- f_{n+1}^{(1)}\right)\right] \tag{A.16}$$

Noting that $v_\perp G/v = \partial F^{(0)}/\partial v_\perp$ and $v_\parallel G/v = \partial F^{(0)}/\partial v_\parallel$, we write the zero-order solutions explicitly,

$$\begin{aligned} f_{\pm 2}^{(0)} &= 0 \\ f_{\pm 1}^{(0)} &= \frac{-e}{2im\Delta_{\pm 1}}\frac{\partial F^{(0)}}{\partial v_\perp}(E_x \mp iE_y) \\ f_0^{(0)} &= \frac{-e}{im\Delta_0}\frac{\partial F^{(0)}}{\partial v_\parallel}E_z \end{aligned} \tag{A.17}$$

To first order we have

$$\begin{aligned} f_{\pm 2}^{(1)} &= \frac{-v_\perp e}{4m\Delta_{\pm 2}}\left\{\frac{\partial}{\partial x}\left(\frac{E_x \mp iE_y}{\Delta_{\pm 1}}\frac{\partial F^{(0)}}{\partial v_\perp}\right) \pm k_y\left(\frac{E_x \mp iE_y}{\Delta_{\pm 1}}\frac{\partial F^{(0)}}{\partial v_\perp}\right)\right. \\ &\qquad \left. \mp \frac{(E_x \mp iE_y)}{\Omega}\frac{\partial F'}{\partial v_\perp}\right\} \\ f_{\pm 1}^{(1)} &= \frac{-v_\perp e}{2m\Delta_{\pm 1}}\left\{\frac{\partial}{\partial x}\left(\frac{E_z}{\Delta_0}\frac{\partial F^{(0)}}{\partial v_z}\right) \pm k_y\left(\frac{E_z}{\Delta_0}\frac{\partial F^{(0)}}{\partial v_z}\right) \mp \frac{E_z}{\Omega}\frac{\partial F'}{\partial v_z}\right\} \\ f_0^{(1)} &= \frac{-v_\perp e}{4m\Delta_0}\left\{\frac{\partial}{\partial x}\left(\left[E_x\left(\frac{1}{\Delta_{-1}} + \frac{1}{\Delta_1}\right) + iE_y\left(\frac{1}{\Delta_{-1}} - \frac{1}{\Delta_1}\right)\right]\frac{\partial F^{(0)}}{\partial v_\perp}\right)\right. \\ &\qquad - 2i\frac{E_y}{\Omega}\left(\frac{\partial F'}{\partial v_\perp} + 2\frac{F'}{v_\perp}\left[1 - \frac{k_z v_z}{\omega}\right]\right) \\ &\qquad \left. + k_y\left(\left[E_x\left(\frac{1}{\Delta_{-1}} - \frac{1}{\Delta_1}\right) + iE_y\left(\frac{1}{\Delta_{-1}} + \frac{1}{\Delta_1}\right)\right]\frac{\partial F^{(0)}}{\partial v_\perp}\right)\right\} \end{aligned} \tag{A.18}$$

and to second order,

$$
\begin{aligned}
f_0^{(2)} = {} & \frac{v_\perp^2 e}{4im\Delta_0}\frac{\partial}{\partial x}\left\{\left(\frac{1}{\Delta_1}+\frac{1}{\Delta_{-1}}\right)\frac{\partial}{\partial x}\left(\frac{E_z}{\Delta_0}\frac{\partial F^{(0)}}{\partial v_z}\right)\right. \\
& \left.+\left(\frac{1}{\Delta_1}-\frac{1}{\Delta_{-1}}\right)\left(\frac{k_y}{\Delta_0}\frac{\partial F^{(0)}}{\partial v_z}-\frac{1}{\Omega}\frac{\partial F'}{\partial v_z}\right)E_z\right\} \\
& -\frac{v_\perp^2 e}{4i\Delta_0 m}k_y\left\{\left(\frac{1}{\Delta_1}-\frac{1}{\Delta_{-1}}\right)\frac{\partial}{\partial x}\left(\frac{E_z}{\Delta_0}\frac{\partial F^{(0)}}{\partial v_z}\right)\right. \\
& \left.+\left(\frac{1}{\Delta_1}+\frac{1}{\Delta_{-1}}\right)\left(\frac{k_y}{\Delta_0}\frac{\partial F^{(0)}}{\partial v_z}-\frac{1}{\Omega}\frac{\partial F'}{\partial v_z}\right)E_z\right\} \\
& -\frac{e}{im\Delta_0\Omega}\left\{\frac{v_\perp^2}{4}\frac{\partial}{\partial x}\left(\frac{1}{\Omega}\frac{\partial F'}{\partial v_z}\right)+\frac{k_y v_z}{\omega}F'\right\}E_z
\end{aligned}
\tag{A.19}
$$

$$
\begin{aligned}
f_{\pm1}^{(2)} = {} & \frac{-ev_\perp}{2i\Delta_{\pm1}m\Omega}\left\{\frac{v_\perp}{8}\frac{\partial}{\partial x}\left(\frac{1}{\Omega}\frac{\partial F'}{\partial v_\perp}\right)(E_x\mp 3iE_y)\right. \\
& \left.\mp i\frac{\partial}{\partial x}\left(\frac{F'}{\Omega}\right)E_y\left(1-\frac{k_z v_z}{\omega}\right)+\frac{F'}{\omega}\left(k_y E_x+i\frac{\partial E_y}{\partial x}\right)\right\} \\
& +\frac{v_\perp^2 e}{8i\Delta_{\pm1}m}\frac{\partial}{\partial x}\left\{\frac{1}{\Delta_{\pm2}}\frac{\partial}{\partial x}\left(\frac{E_x\mp iE_y}{\Delta_{\pm1}}\frac{\partial F^{(0)}}{\partial v_\perp}\right)\right. \\
& \pm\frac{k_y}{\Delta_{\pm2}}\left(\frac{E_x\mp iE_y}{\Delta_{\pm1}}\frac{\partial F^{(0)}}{\partial v_\perp}\right)\mp\frac{E_x\mp iE_y}{\Omega\Delta_{\pm2}}\frac{\partial F'}{\partial v_\perp} \\
& +\frac{1}{\Delta_0}\frac{\partial}{\partial x}\left(\left[E_x\left(\frac{1}{\Delta_{-1}}+\frac{1}{\Delta_1}\right)+iE_y\left(\frac{1}{\Delta_{-1}}-\frac{1}{\Delta_1}\right)\right]\frac{\partial F^{(0)}}{\partial v_\perp}\right) \\
& -\frac{2i}{\Delta_0}\frac{E_y}{\Omega}\left(\frac{\partial F'}{\partial v_\perp}+2\frac{F'}{v_\perp}\left[1-\frac{k_z v_z}{\omega}\right]\right) \\
& \left.+\frac{k_y}{\Delta_0}\left(\left[E_x\left(\frac{1}{\Delta_{-1}}-\frac{1}{\Delta_1}\right)+iE_y\left(\frac{1}{\Delta_{-1}}+\frac{1}{\Delta_1}\right)\right]\frac{\partial F^{(0)}}{\partial v_\perp}\right)\right\} \\
& +\frac{v_\perp^2 e}{8i\Delta_{\pm1}m}k_y\left\{\mp\frac{1}{\Delta_{\pm2}}\frac{\partial}{\partial x}\left(\frac{E_x\mp iE_y}{\Delta_{\pm1}}\frac{\partial F^{(0)}}{\partial v_\perp}\right)\right. \\
& -\frac{k_y}{\Delta_{\pm2}}\left(\frac{E_x\mp iE_y}{\Delta_{\pm1}}\frac{\partial F^{(0)}}{\partial v_\perp}\right)+\frac{E_x\mp iE_y}{\Omega\Delta_{\pm2}}\frac{\partial F'}{\partial v_\perp} \\
& \pm\frac{1}{\Delta_0}\frac{\partial}{\partial x}\left(\left[E_x\left(\frac{1}{\Delta_{-1}}+\frac{1}{\Delta_1}\right)+iE_y\left(\frac{1}{\Delta_{-1}}-\frac{1}{\Delta_1}\right)\right]\frac{\partial F^{(0)}}{\partial v_\perp}\right) \\
& \mp\frac{2i}{\Delta_0}\frac{E_y}{\Omega}\left(\frac{\partial F'}{\partial v_\perp}+2\frac{F'}{v_\perp}\left[1-\frac{k_z v_z}{\omega}\right]\right)\pm\frac{k_y}{\Delta_0}\left(\left[E_x\left(\frac{1}{\Delta_{-1}}-\frac{1}{\Delta_1}\right)\right.\right. \\
& \left.\left.\left.+iE_y\left(\frac{1}{\Delta_{-1}}+\frac{1}{\Delta_1}\right)\right]\frac{\partial F^{(0)}}{\partial v_\perp}\right)\right\}
\end{aligned}
\tag{A.20}
$$

The perturbed current density $\vec{J}$ is

$$J_x = e\int v_x f d^3\vec{v} = \frac{e}{2}\int v_\perp \left(e^{i\phi}+e^{-i\phi}\right)\sum_n f_n e^{in\phi} d^3\vec{v} \tag{A.21}$$

$$J_y = e\int v_y f d^3\vec{v} = \frac{e}{2i}\int v_\perp \left(e^{i\phi}-e^{-i\phi}\right)\sum_n f_n e^{in\phi} d^3\vec{v} \tag{A.22}$$

$$J_z = e\int v_z f d^3\vec{v} = e\int v_z \sum_n f_n e^{in\phi} d^3\vec{v} \tag{A.23}$$

Using $d^3\vec{v} = v_\perp\, dv_\perp\, dv_z\, d\phi$, the ϕ integral picks off the $n = \mp 1$ terms in Eqs (A.21) and (A.22) and the $n = 0$ terms in Eq. (A.23). This gives

$$\begin{aligned} J_x &= \pi e\int v_\perp^2 \left(f_1 + f_{-1}\right) dv_\perp dv_\parallel \\ J_y &= i\pi e\int v_\perp^2 \left(f_1 - f_{-1}\right) dv_\perp dv_\parallel \\ J_z &= 2\pi e\int v_z v_\perp f_0 dv_\perp dv_\parallel \end{aligned} \tag{A.24}$$

Now write these currents explicitly to second order in $\rho = v_\perp/\Omega$ using the solutions in Eqs (A.17)–(A.20). Integrating the $\partial F/\partial v_\perp$ terms by parts, we get $\vec{J} = \vec{J}^{(0)} + \vec{J}^{(1)} + \vec{J}^{(2)}$, where

$$J_x^{(0)} = \frac{\pi e^2}{im}\int v_\perp \left[\left(\frac{1}{\Delta_1}+\frac{1}{\Delta_{-1}}\right)E_x - \left(\frac{1}{\Delta_1}-\frac{1}{\Delta_{-1}}\right)iE_y\right] F^{(0)} dv_\perp dv_z$$

$$J_y^{(0)} = \frac{\pi e^2}{im}\int v_\perp \left[\left(\frac{1}{\Delta_1}-\frac{1}{\Delta_{-1}}\right)iE_x + \left(\frac{1}{\Delta_1}+\frac{1}{\Delta_{-1}}\right)E_y\right] F^{(0)} dv_\perp dv_z$$

$$J_z^{(0)} = \frac{-2\pi e^2}{im}\int \frac{v_z v_\perp}{\Delta_0}\frac{\partial F^{(0)}}{\partial v_\parallel} E_z dv_\perp dv_\parallel$$

$$J_x^{(1)} = \frac{-\pi e^2}{2m}\int v_\perp^3\left[\left(\frac{1}{\Delta_1}+\frac{1}{\Delta_{-1}}\right)\frac{E_z'}{\Delta_0}+\left(\frac{1}{\Delta_1}-\frac{1}{\Delta_{-1}}\right)\frac{k_yE_z}{\Delta_0}\right]\frac{\partial F^{(0)}}{\partial v_z}dv_\perp dv_z$$

$$J_y^{(1)} = \frac{-i\pi e^2}{2m}\int v_\perp^3\left\{\left[\left(\frac{1}{\Delta_1}+\frac{1}{\Delta_{-1}}\right)\frac{k_yE_z}{\Delta_0}\right.\right.$$
$$\left.\left.+\left(\frac{1}{\Delta_1}-\frac{1}{\Delta_{-1}}\right)\frac{E_z'}{\Delta_0}\right]\frac{\partial F^{(0)}}{\partial v_z}-\frac{2E_z}{\Delta_0\Omega}\frac{\partial F'}{\partial v_z}\right\}dv_\perp dv_z$$

$$J_z^{(1)} = \frac{\pi e^2}{m}\int v_zv_\perp\left\{\frac{\partial}{\partial x}\left(\left[\left(\frac{1}{\Delta_{-1}}+\frac{1}{\Delta_1}\right)\frac{E_x}{\Delta_0}+\left(\frac{1}{\Delta_{-1}}-\frac{1}{\Delta_1}\right)\frac{iE_y}{\Delta_0}\right]F^{(0)}\right)\right.$$
$$+k_y\left[\left(\frac{1}{\Delta_{-1}}-\frac{1}{\Delta_1}\right)\frac{E_x}{\Delta_0}+\left(\frac{1}{\Delta_{-1}}+\frac{1}{\Delta_1}\right)\frac{iE_y}{\Delta_0}\right]F^{(0)}$$
$$\left.-\frac{2iE_y}{\Delta_0\Omega}\frac{k_zv_z}{\omega}F'\right\}dv_\perp dv_z$$

For brevity we omit the lengthy expressions for $\vec{J}^{(2)}$.

Assuming $F^{(0)}$ to be Maxwellian,

$$F^{(0)} = \frac{n}{\pi^{\frac{3}{2}}\alpha^3}\exp\left(-\left[\frac{v_\perp^2+v_\parallel^2}{\alpha^2}\right]\right)$$

where $\alpha = \sqrt{2kT/m}$, we can write the integrals over $v_\parallel$ in Eq. (A.24) in terms of the functions $\widetilde{P}_n$ and P_n in Eq. (5); after some tedious algebra, we find the warm plasma current density and conductivity tensor given by Eq. (4). Note that if one ignores all x-dependences except those in $\vec{E}$ and the resonant denominator, $\Delta_{\mp 2}$, then $J_x^{(2)}$ and $J_y^{(2)}$ from Eq. (A.24) reduce to

$$J_x^{(2)} = \frac{\partial}{\partial x}\left\{\frac{-\pi e^2}{2im\Omega^2}\int v_\perp^3 dv_\perp dv_\parallel F^{(0)}\left(\left[\frac{1}{\Delta_2}+\frac{1}{\Delta_{-2}}-\frac{1}{\Delta_1}-\frac{1}{\Delta_{-1}}\right]\frac{\partial E_x}{\partial x}\right.\right.$$
$$\left.\left.+\left[\frac{1}{\Delta_{-2}}-\frac{1}{\Delta_2}+\frac{2}{\Delta_1}-\frac{2}{\Delta_{-1}}\right]\frac{\partial(iE_y)}{\partial x}\right)\right\}$$

$$J_y^{(2)} = \frac{\partial}{\partial x}\left\{\frac{\pi e^2}{2m\Omega^2}\int v_\perp^3 dv_\perp dv_\parallel F^{(0)}\left(\left[\frac{1}{\Delta_{-2}}-\frac{1}{\Delta_2}+\frac{2}{\Delta_1}-\frac{2}{\Delta_{-1}}\right]\frac{\partial E_x}{\partial x}\right.\right.$$
$$\left.\left.+\left[\frac{1}{\Delta_{-2}}+\frac{1}{\Delta_2}-\frac{3}{\Delta_{-1}}-\frac{3}{\Delta_1}+\frac{4}{\Delta_0}\right]\frac{\partial(iE_y)}{\partial x}\right)\right\}$$

which is the result of Chiu and Mau [7] for second harmonic heating. As pointed out in Ref. [7], the effect of the zero-order drift does not enter in this limit. Thus, the present result, Eqs (A.18)–(A.20), includes the second harmonic result of Ref. [7] when the appropriate limit is taken.

REFERENCES

1. ITOH, K., ITOH, S., FUKUYAMA, A., Nucl. Fusion **24** (1984) 13.
2. VILLARD, L., APPERT, K., GRUBER, R., VACLAVIK, J., Comput. Phys. Rep. **4** (1986) 95.
3. PHILLIPS, M. W., TODD, A.M.M., Comput. Phys. Commun. **40** (1986) 65.
4. JAEGER, E. F., BATCHELOR, D. B., WEITZNER, H., WHEALTON, J. H., Comput. Phys. Commun. **40** (1986) 33.
5. ELET, R. S., HWANG, D. Q., PHILLIPS, C. K., Bull. Am. Phys. Soc. **29** (1984) 1336.
6. FUKUYAMA, A., ITOH, K., ITOH, S.-I., Comput. Phys. Rep. **4** (1986) 137.
7. CHIU, S. C., MAU, T. K., Nucl. Fusion **23** (1983) 1613.
8. COLESTOCK, P. L., KASHUBA, R. J., Nucl. Fusion **23** (1983) 763.
9. FUKUYAMA, A., NISHIYAMA, S., ITOH, K., ITOH, S.-I., Nucl. Fusion **23** (1983) 1005.
10. APPERT, K., HELLSTEN, T., VACLAVIK, J., VILLARD, L., Comput. Phys. Commun. **40** (1986) 73.
11. ROMERO, H., SCHARER, J., ICRF Fundamental Minority Heating in Inhomogeneous Tokamak Plasmas, Univ. of Wisconsin, Madison, Rep. ECE-86-5 (1986).
12. FERRARO, R. D., FRIED, B. D., paper 2D31 presented at the 1986 Sherwood Theory Conference: Annual Controlled Fusion Theory Meeting, New York, N.Y., 1986.
13. MARTIN, T., VACLIVIK, J., Dielectric Tensor Operator of a Nonuniformly Magnetized Inhomogeneous Plasma, Ecole Polytechnique Federale, Lausanne, Rep. LRP 259/85 (1985), to be published in Phys. Fluids.
14. SMITHE, D. N., COLESTOCK, P. L., KASHUBA, R. J., KAMMASH, T., private communication (January 29–30, 1987).
15. KAY, A., CAIRNS, R. A., LASHMORE-DAVIES, C. N., in Controlled Fusion and Plasma Heating (Proc. 13th European Conf. Schliersee, 1986), Part 1, European Physical Society (1986) 93.

16. COLESTOCK, P. L., KLUGE, R. F., Bull. Am. Phys. Soc. **27** (1982) 1076; KASHUBA, R. J., SMITHE, D. N., COLESTOCK, P. L., Bull. Am. Phys. Soc. **29** (1984) 1398.

17. FRIED, B. D., CONTE, S. D., The Plasma Dispersion Relation, Academic Press, New York (1961).

18. BERS, A., in Plasma Physics (Université de Grenoble Summer School of Theoretical Physics, Les Houches, 1972) (DEWITT, C., PEYRAUD, J., Eds), Gordon and Breach, New York (1975) 128.

19. COLESTOCK, P. L., private communication (April 16, 1986).

ORNL/TM-10224
Dist. Category UC-20 g

INTERNAL DISTRIBUTION

1. D. B. Batchelor
2. C. O. Beasley
3. B. A. Carreras
4. M. D. Carter
5. E. C. Crume
6. N. O. Dominguez
7. R. A. Dory
8. C. L. Hedrick
9. S. P. Hirshman
10. J. T. Hogan
11. W. A. Houlberg
12. H. C. Howe
13. E. F. Jaeger
14. J-N. Leboeuf
15. G. S. Lee
16. J. F. Lyon
17. J. A. Rome
18. K. C. Shaing
19. J. Sheffield
20. D. A. Spong
21–22. Laboratory Records Department
23. Laboratory Records, ORNL–RC
24. Document Reference Section
25. Central Research Library
26. Fusion Energy Division Library
27–28. Fusion Energy Division Publications Office
29. ORNL Patent Office

EXTERNAL DISTRIBUTION

30. Office of the Assistant Manager for Energy Research and Development, U.S. Department of Energy, Oak Ridge Operations Office, P. O. Box E, Oak Ridge, TN 37831
31. J. D. Callen, Department of Nuclear Engineering, University of Wisconsin, Madison, WI 53706-1687
32. J. F. Clarke, Director, Office of Fusion Energy, Office of Energy Research, ER-50 Germantown, U.S. Department of Energy, Washington, DC 20545
33. R. W. Conn, Department of Chemical, Nuclear, and Thermal Engineering, University of California, Los Angeles, CA 90024
34. S. O. Dean, Fusion Power Associates, 2 Professional Drive, Suite 248, Gaithersburg, MD 20879
35. H. K. Forsen, Bechtel Group, Inc., Research Engineering, P. O. Box 3965, San Francisco, CA 94105
36. J. R. Gilleland, GA Technologies, Inc., Fusion and Advanced Technology, P.O. Box 81608, San Diego, CA 92138
37. R. W. Gould, Department of Applied Physics, California Institute of Technology, Pasadena, CA 91125
38. R. A. Gross, Plasma Research Laboratory, Columbia University, New York, NY 10027
39. D. M. Meade, Princeton Plasma Physics Laboratory, P.O. Box 451, Princeton, NJ 08544
40. M. Roberts, International Programs, Office of Fusion Energy, Office of Energy Research, ER-52 Germantown, U.S. Department of Energy, Washington, DC 20545
41. W. M. Stacey, School of Nuclear Engineering and Health Physics, Georgia Institute of Technology, Atlanta, GA 30332
42. D. Steiner, Nuclear Engineering Department, NES Building, Tibbetts Avenue, Rensselaer Polytechnic Institute, Troy, NY 12181
43. R. Varma, Physical Research Laboratory, Navrangpura, Ahmedabad 380009, India

44. Bibliothek, Max-Planck Institut fur Plasmaphysik, D-8046 Garching, Federal Republic of Germany
45. Bibliothek, Institut fur Plasmaphysik, KFA, Postfach 1913, D-5170 Julich, Federal Republic of Germany
46. Bibliotheque, Centre de Recherches en Physique des Plasmas, 21 Avenue des Bains, 1007 Lausanne, Switzerland
47. F. Prevot, CEN/Cadarache, Departement de Recherches sur la Fusion Controlee, F-13108 Saint-Paul-lez-Durance Cedex, France
48. Documentation S.I.G.N., Departement de la Physique du Plasma et de la Fusion Controlee, Centre d'Etudes Nucleaires, B.P. 85, Centre du Tri, F-38041 Grenoble, France
49. Library, Culham Laboratory, UKAEA, Abingdon, Oxfordshire, OX14 3DB, England
50. Library, FOM-Instituut voor Plasma-Fysica, Rijnhuizen, Edisonbaan 14, 3439 MN Nieuwegein, The Netherlands
51. Library, Institute of Plasma Physics, Nagoya University, Nagoya 464, Japan
52. Library, International Centre for Theoretical Physics, P.O. Box 586, I-34100 Trieste, Italy
53. Library, Laboratorio Gas Ionizatti, CP 56, I-00044 Frascati, Rome, Italy
54. Library, Plasma Physics Laboratory, Kyoto University, Gokasho, Uji, Kyoto, Japan
55. Plasma Research Laboratory, Australian National University, P.O. Box 4, Canberra, A.C.T. 2000, Australia
56. Thermonuclear Library, Japan Atomic Energy Research Institute, Tokai Establishment, Tokai-mura, Naka-gun, Ibaraki-ken, Japan
57. G. A. Eliseev, I. V. Kurchatov Institute of Atomic Energy, P.O. Box 3402, 123182 Moscow, U.S.S.R.
58. V. A. Glukhikh, Scientific-Research Institute of Electro-Physical Apparatus, 188631 Leningrad, U.S.S.R.
59. I. Shpigel, Institute of General Physics, U.S.S.R. Academy of Sciences, Ulitsa Ulitsa Vavilova 38, Moscow, U.S.S.R.
60. D. D. Ryutov, Institute of Nuclear Physics, Siberian Branch of the Academy of Sciences of the U.S.S.R., Sovetskaya St. 5, 630090 Novosibirsk, U.S.S.R.
61. V. T. Tolok, Kharkov Physical-Technical Institute, Academical St. 1, 310108 Kharkov, U.S.S.R.
62. Library, Academia Sinica, P.O. Box 3908, Beijing, China (PRC)
63. D. Crandall, Experimental Plasma Research Branch, Division of Development and Technology, Office of Fusion Energy, Office of Energy Research, ER-542 Germantown, U.S. Department of Energy, Washington, DC 20545
64. N. A. Davies, Office of the Associate Director, Office of Fusion Energy, Office of Energy Research, ER-51 Germantown, U.S. Department of Energy, Washington, DC 20545
65. D. B. Nelson, Director, Division of Applied Plasma Physics, Office of Fusion Energy, Office of Energy Research, ER-54 Germantown, U.S. Depart ment of Energy, Washington, DC 20545
66. E. Oktay, Division of Confinement Systems, Office of Fusion Energy, Office of Energy Research, ER-55 Germantown, U.S. Department of Energy, Washington, DC 20545

67. W. Sadowski, Fusion Theory and Computer Services Branch, Division of Applied Plasma Physics, Office of Fusion Energy, Office of Energy Research, ER-541 Germantown, U.S. Department of Energy, Washington, DC 20545
68. P. M. Stone, Fusion Systems Design Branch, Division of Development and Technology, Office of Fusion Energy, Office of Energy Research, ER-532 Germantown, U.S. Depart ment of Energy, Washington, DC 20545
69. J. M. Turner, International Programs, Office of Fusion Energy, Office of Energy Research, ER-52 Germantown, U.S. Depart ment of Energy, Washington, DC 20545
70. R. E. Mickens, Atlanta University, Department of Physics, Atlanta, GA 30314
71. M. N. Rosenbluth, RLM 11.218, Institute for Fusion Studies, University of Texas, Austin, TX 78712
72. Duk-In Choi, Department of Physics, Korea Advanced Institute of Science and Technology, P.O. Box 150, Chong Ryang-Ri, Seoul, Korea
73. Theory Department Read File, c/o D. W. Ross, University of Texas, Institute for Fusion Studies, Austin, TX 78712
74. Theory Department Read File, c/o R. C. Davidson, Director, Plasma Fusion Center, NW 16-202, Massachusetts Institute of Technology, Cambridge, MA 02139
75. Theory Department Read File, c/o R. White, Princeton Plasma Physics Laboratory, P.O. Box 451, Princeton, NJ 08544
76. Theory Department Read File, c/o L. Kovrizhnykh, Lebedev Institute of Physics, Academy of Sciences, 53 Leninsky Prospect, 117924 Moscow, U.S.S.R.
77. Theory Department Read File, c/o B. B. Kadomtsev, I. V. Kurchatov Institute of Atomic Energy, P.O. Box 3402, 123182 Moscow, U.S.S.R.
78. Theory Department Read File, c/o T. Kamimura, Institute of Plasma Physics, Nagoya University, Nagoya 464, Japan
79. Theory Department Read File, c/o C. Mercier, Departemente de Recherches sur la Fusion Controlee, B.P. No. 6, F-92260 Fontenay-aux-Roses (Seine), France
80. Theory Department Read File, c/o T. E. Stringer, JET Joint Undertaking, Culham Laboratory, Abingdon Oxfordshire, OX14 3DB, England
81. Theory Department Read File, c/o R. Briscoe, Culham Laboratory, Abingdon, Oxfordshire OX14 3DB, England
82. Theory Department Read File, c/o D. Biskamp, Max-Planck-Institut fur Plasmaphysik, D-8046 Garching, Federal Republic of Germany
83. Theory Department Read File, c/o T. Takeda, Japan Atomic Energy Research Institute, Tokai Establishment, Tokai-mura, Naka-gun, Ibaraki-ken, Japan
84. Theory Department Read File, c/o J. Greene, GA Technologies, Inc., P.O. Box 81608, San Diego, CA 92138
85. Theory Department Read File, c/o L. D. Pearlstein, L-630, Lawrence Livermore National Laboratory, P.O. Box 5511, Livermore, CA 94550
86. Theory Department Read File, c/o R. Gerwin, CTR Division, Los Alamos National Laboratory, P.O. Box 1663, Los Alamos, NM 87545
87. C. D. Boley, Fusion Power Program, Bldg. 207C, Argonne National Laboratory, Argonne, IL 60439
88. C. De Palo, Library, Associazione EURATOM-ENEA sulla Fusione, CP 65, I-00044 Frascati (Roma), Italy

89. P. H. Diamond, Institute for Fusion Studies, University of Texas, Austin, TX 78712
90. Yu. N. Dnestrovskij, I. V. Kurchatov Institute of Atomic Energy, P.O. Box 3402, 123182 Moscow, U.S.S.R.
91. A. Fruchtman, Courant Institute of Mathematical Physics, New York University, 251 Mercer Street, New York, NY 10012
92. J. Gaffey, IPST, University of Maryland, College Park, MD 20742
93. R. J. Hawryluk, Princeton Plasma Physics Laboratory, P.O. Box 451, Princeton, NJ 08544
94. D. G. McAlees, Advanced Nuclear Fuels Corporation, 600 108th Avenue N.E., Bellevue, WA 98009
95. W. W. Pfeiffer, GA Technologies, Inc., P.O. Box 85608, San Diego, CA 92138
96. D. E. Post, Princeton Plasma Physics Laboratory, P.O. Box 451, Princeton, NJ 08544
97. P. J. Reardon, Princeton Plasma Physics Laboratory, P.O. Box 451, Princeton, NJ 08544
98. K. Riedel, Courant Institute of Mathematical Physics, New York University, 251 Mercer Street, New York, NY 10012
99. A. Ware, Department of Physics, University of Texas, Austin, TX 78712
100. H. Weitzner, Courant Institute of Mathematical Physics, New York University, 251 Mercer Street, New York, NY 10012
101. J. Wiley, Institute for Fusion Studies, University of Texas, Austin, TX 78712
102. S. K. Wong, GA Technologies, Inc., P.O. Box 85608, San Diego, CA 92138
103. S. Yoshikawa, Princeton Plasma Physics Laboratory, P.O. Box 451, Princeton, NJ 08544

104-244. Given distribution as shown in TIC-4500, Magnetic Fusion Energy (Category Distribution UC-20 g: Theoretical Plasma Physics)